iScience

CellPress
OPEN ACCESS

Article

L-lactate exerts a pro-proliferative effect on adult hippocampal precursor cells *in vitro*

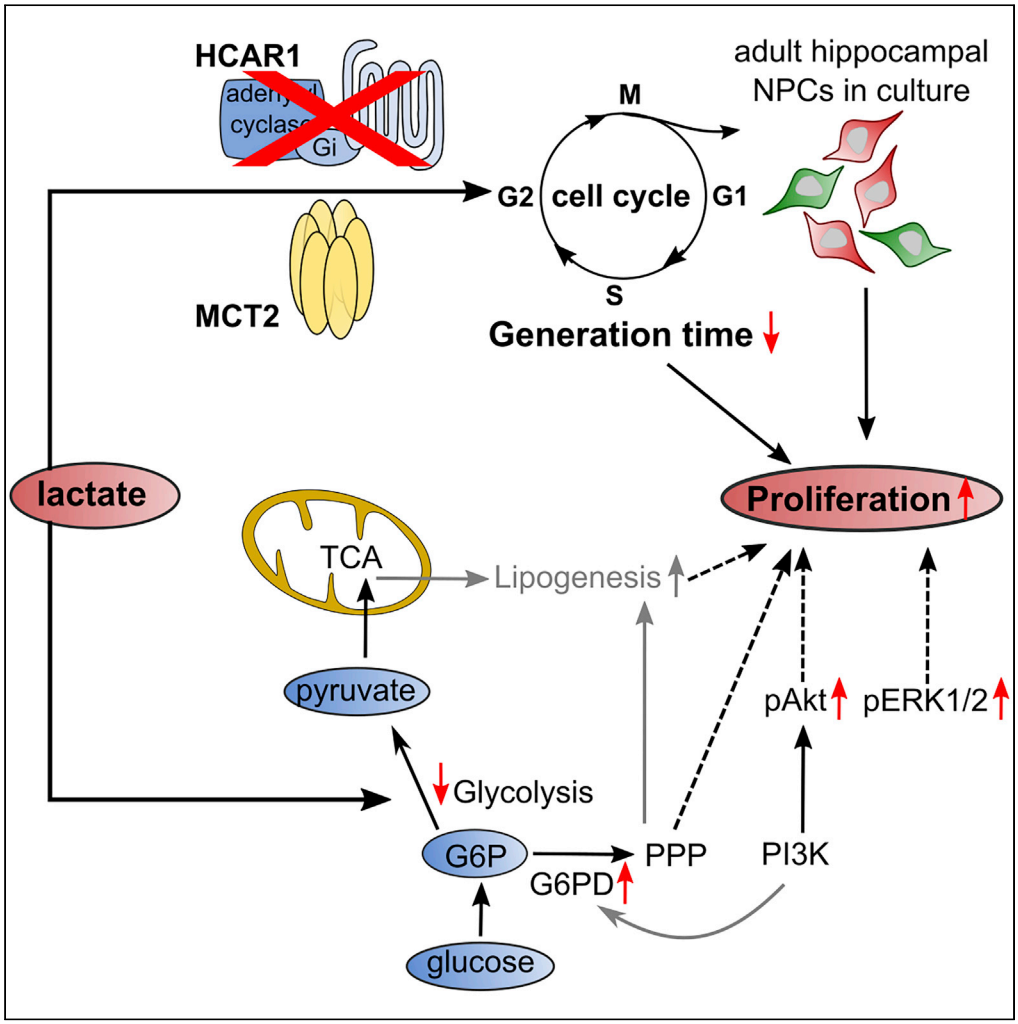

Alexandra Pötzsch, Sara Zocher, Stefanie N. Bernas, Odette Leiter, Annette E. Rünker, Gerd Kempermann

gerd.kempermann@dzne.de

HIGHLIGHTS

L-lactate increases NPC proliferation in an MCT-dependent manner

The pro-proliferative effect of L-lactate is independent of HCAR1 signaling

L-lactate decreases glycolysis in favor of pentose phosphate pathway activity

L-lactate treatment leads to a transient increase in Akt and ERK1/2 phosphorylation

Pötzsch et al., iScience *24*, 102126
February 19, 2021 © 2021
https://doi.org/10.1016/j.isci.2021.102126

iScience

CellPress
OPEN ACCESS

Article

L-lactate exerts a pro-proliferative effect on adult hippocampal precursor cells *in vitro*

Alexandra Pötzsch,[1,2] Sara Zocher,[1,2] Stefanie N. Bernas,[1,2] Odette Leiter,[2] Annette E. Rünker,[1,2] and Gerd Kempermann[1,2,3,*]

SUMMARY

L-lactate has energetic and signaling properties, and its availability is modulated by activity-dependent stimuli, which also regulate adult hippocampal neurogenesis. Studying the effects of L-lactate on neural precursor cells (NPCs) *in vitro*, we found that L-lactate is pro-proliferative and that this effect is dependent on the active lactate transport by monocarboxylate transporters. Increased proliferation was not linked to amplified mitochondrial respiration. Instead, L-lactate deviated glucose metabolism to the pentose phosphate pathway, indicated by increased glucose-6-phosphate dehydrogenase activity while glycolysis decreased. Knockout of *Hcar1* revealed that the pro-proliferative effect of L-lactate was not dependent on receptor activity although phosphorylation of ERK1/2 and Akt was increased following L-lactate treatment. Together, we show that availability of L-lactate is linked to the proliferative potential of NPCs and add evidence to the hypothesis that lactate influences cellular homeostatic processes in the adult brain, specifically in the context of adult hippocampal neurogenesis.

INTRODUCTION

Adult hippocampal neurogenesis describes the continuous generation of new neurons from adult neural stem cells (Kempermann et al., 2004) and presents a unique form of activity-dependent brain plasticity that contributes to hippocampus-dependent learning and cognition (Kempermann et al., 1997; van Praag et al., 1999a, 1999b; Dupret et al., 2007; Lafenêtre et al., 2010; Garthe et al., 2016). The process of adult neurogenesis is strongly regulated by the hippocampal niche as neural stem cells and their progeny can sense, respond, and adapt to extrinsic stimuli (Kempermann 2011). The balance between self-renewal, proliferation, and differentiation is maintained by the sensibility of neural stem and progenitor cells to a multitude of signaling factors in their niche (Scadden 2006; Guilak et al., 2009). Systemic interventions, such as physical activity and learning paradigms, affect the niche microenvironment and positively influence adult neurogenesis (Kempermann, 2015). However, we lack detailed information on how these system-level changes are translated to the neural precursor cells (NPCs) residing in the hippocampus. In this context, the availability of metabolites (Cavallucci et al., 2016) and the cellular energetic state (Knobloch et al., 2013; Beckervordersandforth et al., 2017) represent important factors that have an effect on NPC behavior and plasticity in the adult hippocampus and are potentially modifiable by "lifestyle interventions", such as exercise. In this context, the beneficial effects of exercise and learning stimuli on adult hippocampal neurogenesis have been positively associated to the availability of the metabolite L-lactate (El Hayek et al., 2019; Lev-Vachnish et al., 2019). L-lactate is one of the most common metabolites in the mammalian body and is exchanged between cells and tissues depending on glycolytic and oxidative rates (Brooks 2009). The concentration of L-lactate in the brain is highly activity dependent and can rapidly rise due to either local lactate production by astrocytes or elevated blood lactate that is crossing the blood-brain barrier via the monocarboxylate transporter (MCT) 1 (Rouach et al., 2008; van Hall et al., 2009; Lauritzen et al., 2014; Matsui et al., 2017). Although glucose remains the major energy source for the adult brain, neurons also utilize astrocyte-derived L-lactate as an energetic substrate for oxidative phosphorylation to meet their high energetic demand upon activation, a process described as the astrocyte-neuron lactate shuttle hypothesis (ANLSH; Pellerin and Magistretti 1994; Bouzier-Sore et al., 2006; Bélanger et al., 2011). The ANLSH postulates that L-lactate generated by astrocytes is transported via membrane transporter MCT4 into the extracellular space from which it is imported by neurons through MCT2 and subsequently converted to pyruvate by lactate

[1]German Center for Neurodegenerative Diseases (DZNE) Dresden, Dresden, Germany

[2]CRTD – Center for Regenerative Therapies Dresden, Technische Universität Dresden, Dresden, Germany

[3]Lead contact

*Correspondence: gerd.kempermann@dzne.de

https://doi.org/10.1016/j.isci.2021.102126

dehydrogenase, thereby serving as a substrate for energy metabolism and anabolic pathways (Rafiki et al., 2003; Pellerin et al., 2005; Hashimoto et al., 2008; Mächler et al., 2016). Relatedly, L-lactate trafficking is important for hippocampus-dependent memory formation (Suzuki et al., 2011) and the induction of plasticity-related gene expression, such as c-fos, arc, or zif268, through a modulation of *N*-Methyl-D-aspartate (NMDA) receptor activity in neurons (Yang et al., 2014). Moreover, L-lactate influences neurovascular coupling by mediating vasodilation through vascular endothelial growth factor (Morland et al., 2017) and is linked to the regulation of brain blood flow (Gordon et al., 2008). These latter findings suggest that the effect of L-lactate on plasticity might to some degree be independent of its ability to act as an energetic substrate and imply that L-lactate might have additional intercellular signaling properties. Indeed, the formerly orphan G-protein-coupled receptor GPR81, also known as hydroxycarboxylic acid receptor 1 (HCAR1), can be activated by L-lactate (Lee et al., 2001; Cai et al., 2008; Liu et al., 2009) and modulates the activity of cortical neurons (Bozzo et al., 2013). HCAR1 is expressed in various brain regions, including principal neurons in the neocortex, the cerebellum, and the hippocampus (Lauritzen et al., 2014). On hippocampal slices, L-lactate caused a reduction of cyclic adenosine monophosphate consistent with canonical activation of HCAR1 (Schurr et al., 1988; Lauritzen et al., 2014). In addition, a very high density of HCAR1 in the brain was observed at excitatory synapses in the hippocampus indicating that HCAR1-mediated action of lactate may link synaptic plasticity and energy metabolism (Bergersen 2015). Thus, L-lactate is likely a molecule that exerts both metabolic and signaling functions. However, the exact mechanisms and relative contributions of both mechanisms remain unknown and are likely not universal but context specific.

In this work, we investigated whether changes in the availability of L-lactate might influence hippocampal NPC behavior and present L-lactate as a substrate and signaling molecule with the potential to mediate activity-dependent adaptions of adult hippocampal neurogenesis. Utilizing L-lactate as a proxy for activity *in vitro*, we first examined which processes (NPC activation, proliferation, or differentiation) in the course of adult hippocampal neurogenesis are sensitive to L-lactate treatment. Secondly, we analyzed if MCT-dependent transport and activation of HCAR1 are necessary to induce L-lactate-mediated changes in cellular behavior. Furthermore, we investigated how L-lactate influences energy metabolism and whether it serves as an energetic substrate for NPCs analogous to the ANLSH. We also studied whether any effect of L-lactate was dependent on HCAR1. Finally, we assessed if intracellular signaling, namely Akt and ERK1/2 signaling, was induced by extracellular L-lactate.

RESULTS

L-lactate increases proliferation and shortens the generation time of NPCs

To elucidate whether increased availability of L-lactate affects adult hippocampal neurogenesis and to dissect the mechanistic effects of L-lactate *in vitro*, we utilized two well-established cell culture systems of isolated adult NPCs, neurospheres and adherent monolayer cells (Reynolds and Weiss 1992; Palmer et al., 1995; Ray et al., 1995; Babu et al., 2007). Application of physiological concentrations of L-lactate to NPC cultures from the adult hippocampus stimulated the generation of primary neurospheres and the proliferation of adherent cells in a dose-dependent manner (Figures 1A and 1B). For neurospheres, significant effects on the number of spheres were seen at $\geq$ 5 mM (one-way analysis of variance, ANOVA [$F(3,16) = 3.651$, $p = 0.0353$], $n = 5$; Dunnett's *post hoc*, 2 mM: $p = 0.3$; 5 mM: $p = 0.05$; 10 mM: $p = 0.02$). The distribution of sphere sizes was not affected (Figure S1), indicating that L-lactate could activate NPCs to proliferate and form spheres but did not further stimulate their growth. Adherent cells already responded with a significant increase in BrdU-positive cells after treatment with $\geq$2 mM L-lactate (one-way ANOVA [$F(6,28) = 8.352$, $p < 0.0001$], $n = 5$; Dunnett's *post hoc*, 2 mM: $p = 0.035$; 5 mM: $p = 0.001$; 10 mM: $p = 0.0001$; 20 mM: $p < 0.0001$) demonstrating that physiological concentrations of L-lactate increase NPC proliferation. The pro-proliferative effect was specific to L-lactate as neither D-lactate (the stereoisomer of L-lactate) nor pyruvate (as a related monocarboxylate) induced a change in proliferation under otherwise identical experimental conditions (Figure S1). Moreover, the augmented proliferation was not accompanied by a change in cell death: no cytotoxic effect of L-lactate was found (Figure 1C). Propidium iodide (PI)-based cell cycle analysis (Figures 1D–1I) corroborated our findings as the number of cells in S-phase was significantly increased relative to control cultures at L-lactate concentrations of $\geq$2 mM (one-way ANOVA [$F(4,15) = 18.9$, $p < 0.0001$], $n = 4$; Dunnett's *post hoc*, 2 mM: $p = 0.003$; 5 mM, 10 mM, and 20 mM $p < 0.0001$; Figure 1E). Using an 5-ethynyl-2′-deoxyuridine (EdU)/4′,6-diamidino-2-phenylindole (DAPI) assay for cell cycle phase analysis, we additionally validated the PI-based finding (Figure S2). Furthermore, live cell imaging and semi-automated tracking of individual adherent NPCs (>100 cells per condition) showed an increase in the percentage of dividing cells from 31.37% of control NPCs to 41.75% and 38.83% upon treatment with 5 mM and 20 mM L-lactate, respectively (Figure 1J). From the cells that divided at least two times during the tracking period, we then calculated generation trees (Figure 1K). These allowed us to determine the time between

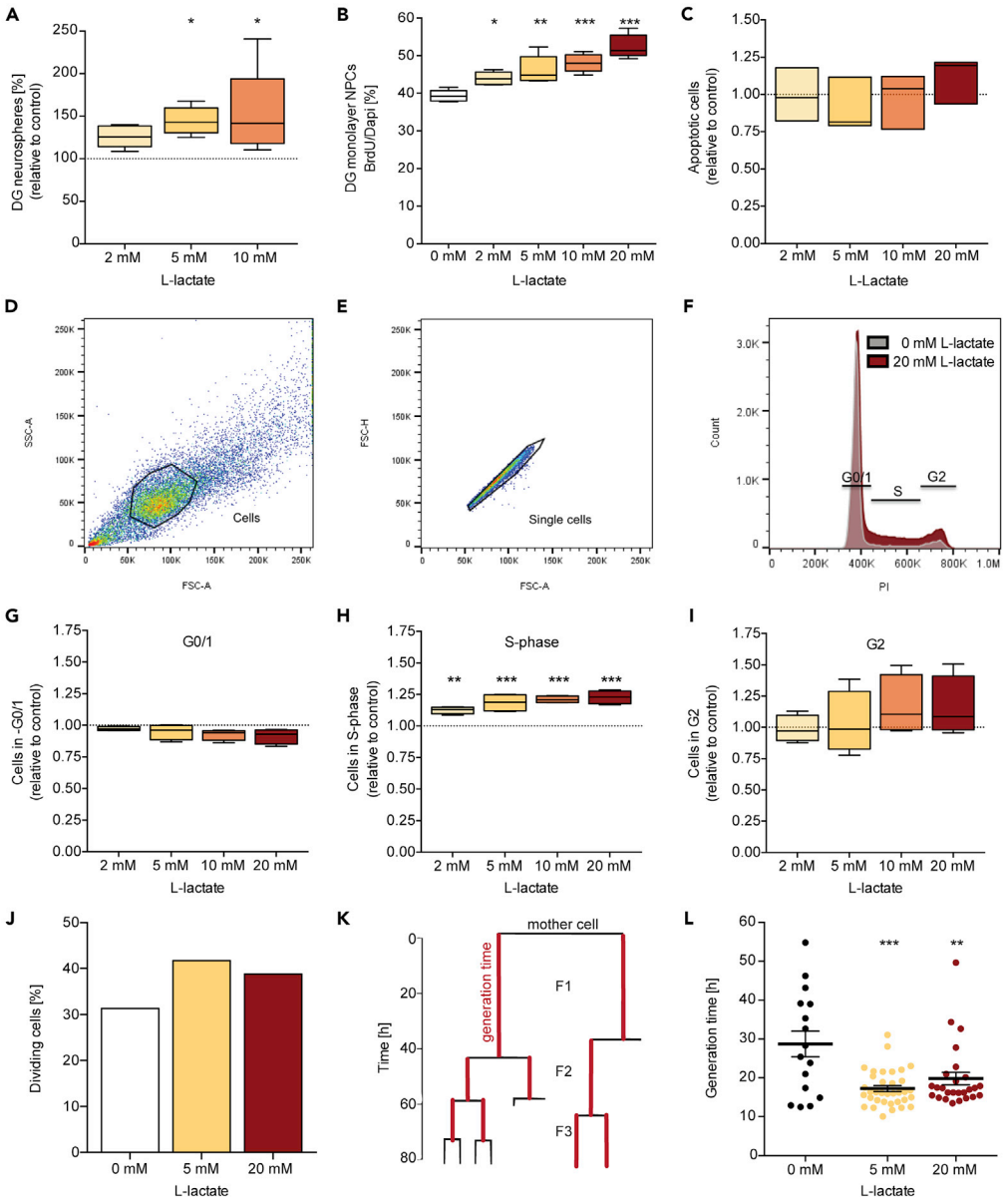

Figure 1. L-lactate increases proliferation of hippocampal NPCs through shortening of the generation time

(A) Relative amount of neurospheres generated from NPCs derived from the dentate gyrus following 10 days of L-lactate treatment (n = 5).

(B) Percentages of BrdU-positive monolayer NPCs generated from the dentate gyrus after 48 hr of L-lactate supplementation (n = 5).

(C) No occurrence of apoptosis 48 hr after L-lactate treatment in monolayer NPCs expressed relative to control (n = 3).

(D–F) Representation of gating strategy and determination of cell cycle phases.

(G–I) PI-based cell cycle analysis of monolayer NPCs following 48 hr of L-lactate treatment presented relative to control (n = 5).

(J) Percentages of dividing cells calculated from one life tracking experiment (images acquired every 5 min for 3.5 days) of L-lactate-treated monolayer NPCs. In total, at least 100 cells per treatment group were analyzed.

(K) Representative generation tree of one mother cell and all of the subsequently tracked later generations (F1, F2, F3). Marked in red the time between cell divisions, termed generation time.

(L) Generation times of cells that divided at least two times during the 3.5 days of live cell tracking (n = 16 for 0 mM, n = 35 for 5 mM, n = 26 for 20 mM L-lactate).

Statistics: one-way ANOVA with Dunnett's *post hoc*; *p < 0.05, **p < 0.01, ***p < 0.001.

each cell division (generation time, marked in red) for every progeny of the first mother cell (F1, F2, F3, etc.). The generation times calculated from the tracking data further revealed that the time between cell divisions was significantly decreased (one-way ANOVA [$F(2,74) = 10.81$, $p < 0.0001$], Dunnett's *post hoc*) from 28.72 ± 3.25 hr ($n = 16$) in control cells to 17.24 ± 0.78 hr (5 mM: $p < 0.0001$; $n = 35$) and 19.83 ± 1.59 hr (20 mM, $p = 0.002$; $n = 26$) in L-lactate conditions indicating that the increase in proliferation was linked to a shortened generation time (Figure 1L).

Subventricular zone -derived precursor cells do not respond to L-lactate

Besides the hippocampus, the adult brain harbors a second neurogenic niche in the subventricular zone (SVZ) of the lateral ventricles. As a number of studies have demonstrated that the stem and precursor cells residing in the hippocampal and subventricular niches react differently to external stimuli (Walker et al., 2008; Leiter et al., 2019), we analyzed whether the pro-proliferative effect of L-lactate on dentate gyrus-(DG)-derived NPCs is shared by precursor cells isolated from the SVZ or if the increase in proliferation is a hippocampal precursor-specific phenomenon. We found that NPCs isolated from the adult SVZ did not respond to L-lactate treatment, and no effects on cell proliferation were found in both neurosphere and adherent cell cultures (Figures 2A and 2B). We further discovered that the expression of the L-lactate transporters *Slc16a1* (MCT1), *Slc16a7* (MCT2), and *Slc16a3* (MCT4) was not statistically different between NPCs generated from the SVZ and DG ($n = 5$, Figures 2F and 2G). Moreover, we verified by Western blot that, NPCs from the SVZ express HCAR1 at the protein level (Figure 2H). Based on these findings, we conclude that even though NPCs of the DG and SVZ both express L-lactate transporters and the receptor HCAR1, only DG-derived NPCs are sensitive to environmental changes of L-lactate. This might indicate a specific function of L-lactate for adult hippocampal precursor cells.

L-lactate does not induce proliferation in BMP4-treated NPCs

Within certain limits, NPCs in culture represent a heterogeneous pool of proliferating precursor cells at different developmental stages. Quiescence and re-activation of quiescent cells can be modeled in adherent NPCs with BMP4 (Martynoga et al., 2013; Figure 2C). Thus, we next analyzed whether L-lactate could stimulate non-cycling NPCs to enter proliferation. Following supplementation of BMP4-treated cells with L-lactate, we found that L-lactate did not induce a substantial amount of proliferation (<0.02% of cells BrdU-positive; $n = 3$; Figure 2D). Only after BMP4-treated cells had been stimulated to re-enter the cell cycle by re-application of FGF2 and EGF, did co-treatment with L-lactate augment proliferation as evidenced by a significant increase in BrdU-positive cells (one-way ANOVA [$F(2,6) = 13.52$, $p = 0.006$], $n = 3$; Dunnett's *post hoc*, 5 mM: $p = 0.012$; 20 mM: $p = 0.005$; Figure 2E). Analysis of transporter expression further revealed that *Slc16a1* (MCT1; one-way ANOVA [$F(2,12) = 36.49$, $p < 0.0001$], $n = 5$; Dunnett's *post hoc*, $p < 0.0001$) and *Slc16a3* (MCT4; one-way ANOVA [$F(2,12) = 14.35$, $p = 0.0007$], $n = 5$; Dunnett's *post hoc*, $p = 0.0005$) are significantly higher expressed in BMP4-treated NPCs as compared to proliferating cells (Figures 2F and 2G) indicating that they are adapted to shuttle L-lactate out of the cell into the extracellular space. In addition, we showed that BMP4-treated cells also express HCAR1 at the protein level (Figure 2H). Together, these data suggest that increased extracellular availability of L-lactate does not result in recruitment of quiescent NPCs and imply that increased expression of L-lactate exporters might be responsible for their lack of responsiveness.

Neuronal fate determination is not affected by L-lactate

Differentiation of NPCs is associated with a switch from mostly glycolytic to mitochondrial energy production (Xu et al., 2013; Shin et al., 2015; Wanet et al., 2015; Beckervordersandforth et al., 2017). Since the ANLSH suggested L-lactate to be a precursor for mitochondrial respiration in neurons, we hypothesized that L-lactate would influence differentiation in favor of neuronal as opposed to astrocytic fate determination. The induction of differentiation of L-lactate-treated neurospheres, however, did not change the percentage of βIII-tubulin-positive cells (Figures 3A–3C). In addition, supplementation of adherent NPCs with L-lactate at the onset of differentiation did not influence the potential for neuronal differentiation, as we did not detect significant differences in Map2ab-positive cells (Figures 3D–3F). This suggests that, at least in the here presented assays, L-lactate specifically potentiates the proliferative behavior of hippocampal NPCs but does not affect their differentiation *in vitro*.

MCT transport is crucial for the pro-proliferative effect of L-lactate

Expression of MCTs was reported to be sensitive to systemic interventions resulting in increased expression of MCT2 in the hippocampus following acute physical exercise (Takimoto and Hamada 2014; Matsui

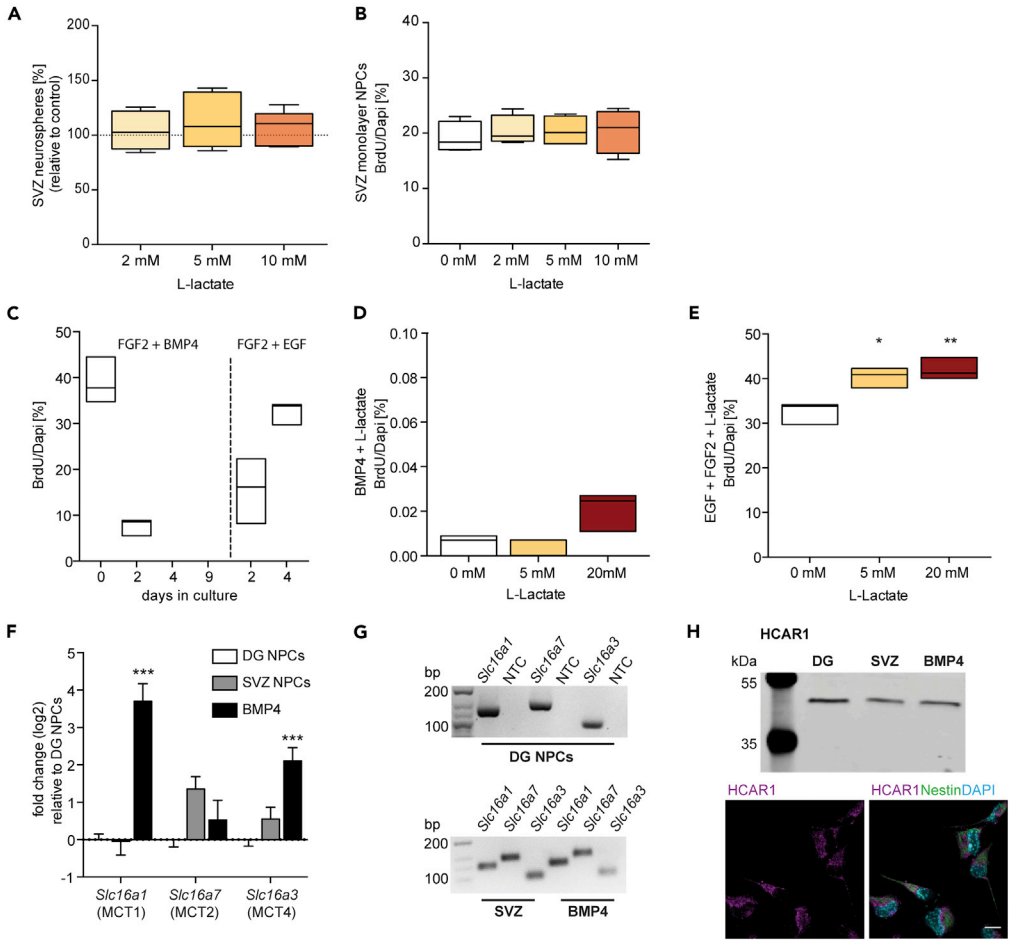

Figure 2. Effect of L-lactate is specific to proliferating hippocampal NPCs

(A) Neurospheres generated from NPCs of the SVZ after 10 days of treatment with L-lactate relative to control (n = 5).

(B) Percentage of BrdU-positive monolayer NPCs derived from the SVZ after 48 hr of L-lactate treatment (n = 5).

(C) Quantification of BrdU-positive cells following induction of quiescence with BMP4 and subsequent re-activation upon BMP4 withdrawal and treatment with FGF2 + EGF under control conditions (n = 3).

(D) Percentages of BrdU-positive cells in BMP4-induced quiescent NPCs co-treated with L-lactate. Data are shown as mean ± standard error of the mean (SEM; n = 3).

(E) BMP4-induced quiescent NPCs were stimulated to re-enter proliferation following re-plating and treatment with EGF and FGF2. Percentages of BrdU-positive cells upon co-treatment with L-lactate during stimulation (n = 3).

(F) Expression analysis of L-lactate transporters in BMP4-treated NPCs from DG and SVZ-derived cells relative to untreated NPCs generated from the DG (n = 5).

(G) Products of quantitative polymerase chain reactions (qPCRs) verifying correct amplification (NTC: non-template control).

(H) Western blot of HCAR1 in DG, SVZ, and BMP4-treated NPCs and representative image of HCAR1-positive NPCs co-stained for nestin and DAPI. Scale bar, 10 μm.

Bar graphs represent mean ± SEM. Statistics: one-way ANOVA with Dunnett's *post hoc*; *p < 0.05, **p < 0.01, ***p < 0.001.

et al., 2017), which suggests a concomitantly increased uptake of L-lactate by hippocampal cells. Consequently, we next investigated the importance of MCT-dependent L-lactate transport in hippocampal NPCs. Therefore, we first aimed to demonstrate that all three MCT transporters are also expressed at the protein level. However, here we could only verify expression of MCT2 and MCT4 by both Western blot and immunostainings (Figures 4A and 4B). Next, we applied the global MCT inhibitor α-cyano-4-hydroxy-cinnamate (4-CIN) to our NPCs. As MCTs also transport pyruvate across cell membranes, we initially demonstrated that the inhibitor alone had no effect on baseline proliferation to exclude that 4-CIN could

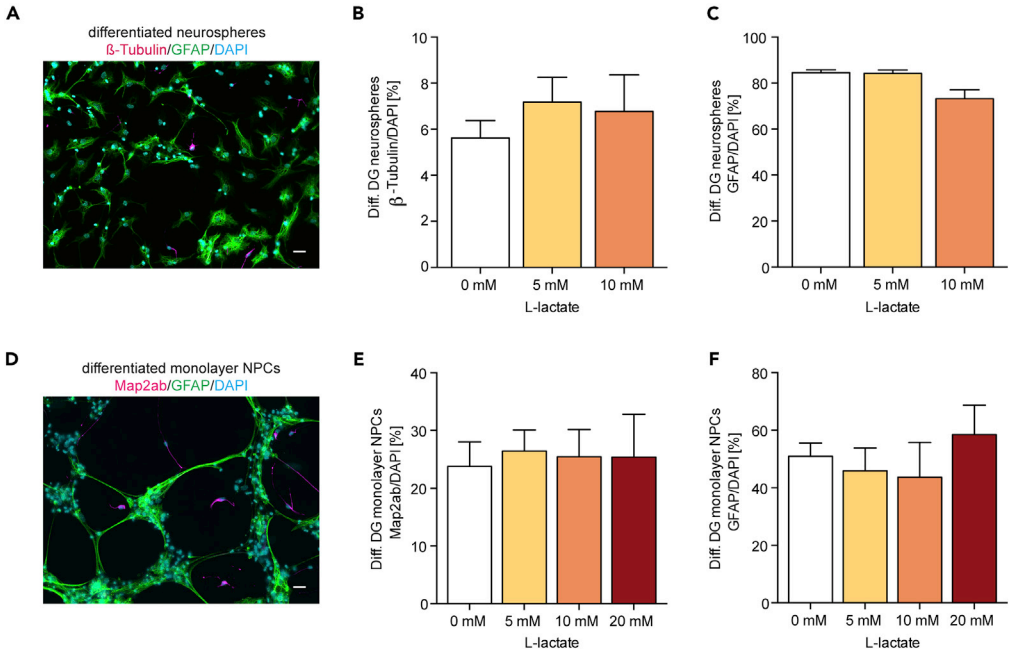

Figure 3. L-lactate does not promote neuronal fate determination *in vitro*

(A) Representative image of differentiated neurospheres stained with antibodies against β-tubulin for neuronal and GFAP for astrocytic fate determination. Scale bar, 20 μm.

(B and C) Quantification of neurons and astrocytes in differentiated neurospheres following L-lactate treatment (n = 3).

(D) Representative image of differentiated adherent NPCs stained with antibodies against Map2ab for neuronal and GFAP for astrocytic fate determination. Scale bar, 20 μm.

(E and F) Quantification of neurons and astrocytes in differentiated monolayer NPCs in response to L-lactate supplementation (n = 3).

Bar graphs represent mean ± standard error of the mean (SEM).

impair proliferation through general inhibition of monocarboxylate transport (Figure S3). Conveniently, 4-CIN displays different affinities for MCT1, 2, and 4 (Bröer et al., 1999; Erlichman et al., 2009) and thus, depending on concentration, can be used to discern the relative contribution of the individual L-lactate transporters (Figures 4C–4F). Complete inhibition of MCT2 (100 μM 4-CIN; n = 3) and only partial inhibition of MCT1, whose expression could not be shown conclusively at the protein level, reduced the pro-proliferative effect of L-lactate to a very small, statistically insignificant increase (Figure 4D). Further raising 4-CIN concentrations (400 μM and 800 μM; n = 3) completely diminished this residual small effect of L-lactate and proliferation remained at baseline levels (Figures 4E and 4F). Together, this indicates that MCT-mediated transport of L-lactate plays a crucial role in stimulating proliferation and implicates that L-lactate could serve as a substrate for metabolic pathways.

L-lactate deviates glucose metabolism while mitochondrial respiration remains at baseline levels

L-lactate is mostly known as the end product of glycolysis that, according to the ANLSH, can be used as an energetic substrate for mitochondrial respiration. Thus, we hypothesized that extracellular L-lactate availability likely influences cellular energy metabolism and that an increase in oxidative phosphorylation would be linked to the observed pro-proliferative effect of L-lactate.

First, we analyzed whether L-lactate influenced glucose metabolism and could show that treatment with L-lactate (20 mM) resulted in a significantly decreased glycolytic output compared to controls ([t(4) = 6.989, p = 0.002]; n = 3; Figures 5A and 5B). The same effect was seen in cultures that were treated with L-lactate 24 hr before the analysis of metabolism was performed (Figure S4). Interestingly, however, the consumption of glucose from the culture medium was not different between treated and non-treated cells (Figure 5C), implying that an alternate route for glucose metabolism exists in L-lactate-treated NPCs. Accordingly, activity of G6PD, key enzyme of the first irreversible step of the pentose phosphate pathway

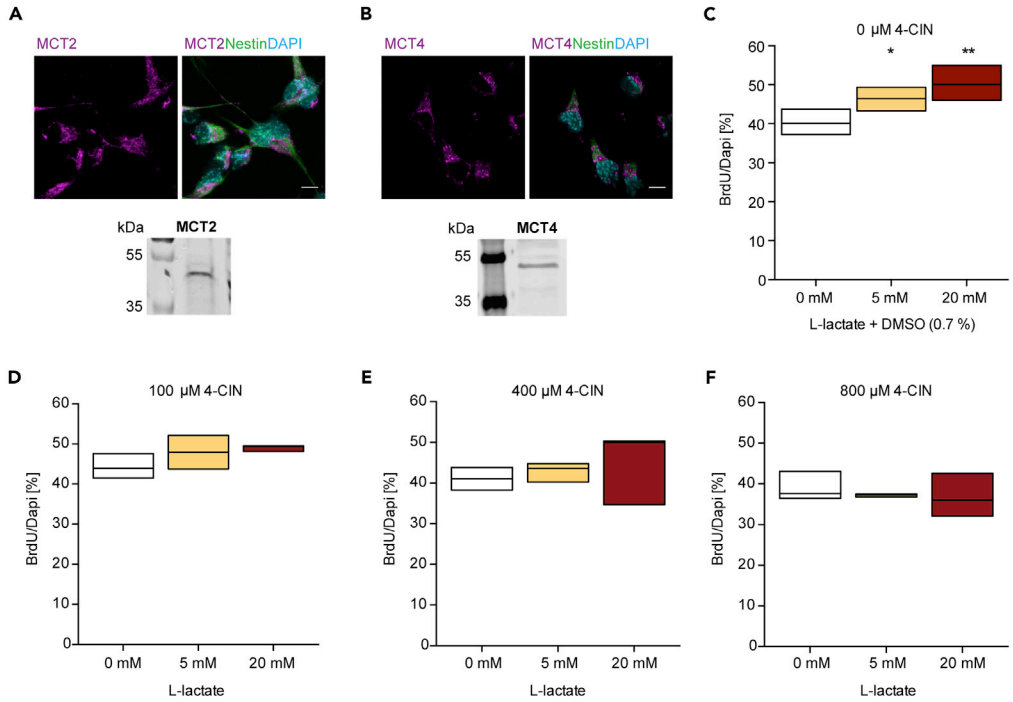

Figure 4. MCT transport is required for the pro-proliferative effect of L-lactate

(A and B) Representative western blots and images of MCT2 and MCT4-positive monolayer NPCs co-labeled with nestin and DAPI. Scale bar, 10 µm.

(C) Percentages of BrdU-positive cells following treatment with 0 µM 4-CIN: control condition to D – F (n = 3).

(D) Percentages of BrdU-positive cells following treatment with 100 µM 4-CIN leading to complete inhibition of MCT2 (100%) and only partial inhibition of MCT1 (~12.5%) and MCT4 (~1%) transport (n = 3).

(E) Percentages of BrdU-positive cells following inhibition of MCT2 (100%), MCT1 (~50%), and MCT4 (~25%) after treatment with 400 µM 4-CIN (n = 3).

(F) Percentages of BrdU-positive cells after complete inhibition of MCT-mediated L-lactate uptake following application of 800 µM 4-CIN (n = 3). Statistics: one-way ANOVA with Dunnett's *post hoc*; *p < 0.05, **p < 0.01.

(PPP), was significantly increased upon supplementation with 20 mM L-lactate (6 hr: [t(4) = 5.598, p = 0.005]; 24 hr: [t(4) = 4.826, p = 0.008]; 48 hr: [t(4) = 4.047, p = 0.01]; n = 3; Figure 5D). These data suggest that NPCs react to exogenous L-lactate by partly directing glucose toward the PPP instead of glycolysis, confirming a proposed link between augmented PPP activity and proliferative behavior (Tian et al., 1998; Jiang et al., 2011; Xu et al., 2016). Next, we investigated whether L-lactate increased mitochondrial respiration. To our surprise, extracellular L-lactate (20 mM) had no positive effect on oxidative phosphorylation (Figure 5E) and respiration remained at baseline levels (n = 3; Figure 5F).

Taken together, we thus show that the increased proliferation after exposure to L-lactate is not associated with augmented mitochondrial respiration and, hence, the use of L-lactate as an energetic substrate as suggested by the ANLSH. This would not, however, exclude the utilization of L-lactate in other anabolic processes, such as *de novo* lipogenesis. Moreover, in our hands treatment with L-lactate resulted in decreased glycolysis and increased G6PD activity suggesting enhanced PPP activity. This indicates that either L-lactate inhibits its own production via a feedback mechanism or that the changes in glucose metabolism are mediated through intracellular signaling cascades induced by L-lactate.

The pro-proliferative effect of L-lactate is not dependent on HCAR1

We next investigated whether the effect of L-lactate is solely due to its function as an intracellular substrate or if, additionally, HCAR1-mediated signaling properties are necessary for inducing proliferation. Initially, we supplemented cells with the HCAR1-agonist 3,5-DHBA to analyze whether receptor activation alone could increase proliferation. However, treatment with increasing concentrations of 3,5-DHBA did not induce proliferation of NPCs (n = 5; Figure 6A), suggesting that HCAR1 is not involved or that its activation

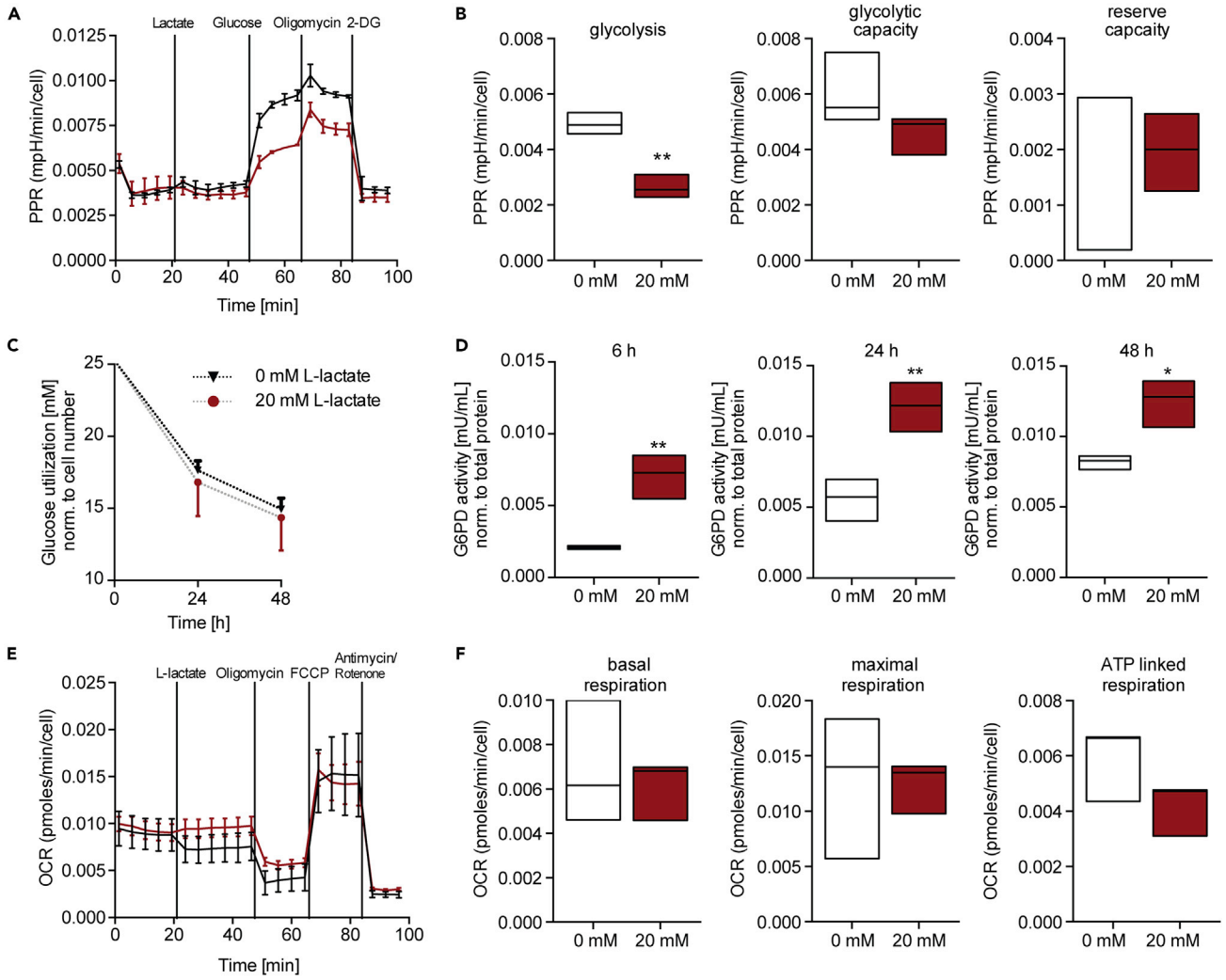

Figure 5. L-lactate deviates glucose metabolism while mitochondrial respiration remains at baseline levels

(A) Glycolytic behavior of NPCs following subsequent manipulation of metabolism with L-lactate (0 mM or 20 mM), glucose, oligomycin, and 2-deoxy-glucose (2-DG) using the Seahorse Analyzer XF96. Data are normalized to total cell numbers and expressed as proton production rate (PPR) (n = 3).

(B) Rate of glycolysis, glycolytic capacity, and reserve capacity in the absence or presence of L-lactate (n = 3).

(C) Glucose in cell culture media after 24 hr and 48 hr of culture following L-lactate treatment (n = 3).

(D) Activity of G6PD after 6 hr, 24 hr, and 48 hr of stimulation with L-lactate (0 mM or 20 mM). Data normalized to total protein concentration (n = 3).

(E) Mitochondrial respiration of NPCs presented as oxygen consumption rate (OCR) and normalized to total cell numbers following treatment with L-lactate (0 mM or 20 mM), oligomycin, carbonyl cyanide-4 (trifluoromethoxy) phenylhydrazone (FCCP), and antimycin/rotenone analyzed with the Seahorse Analyzer XF96 (n = 3).

(F) Rate of basal respiration, maximal respiration, and ATP-linked respiration in the absence or presence of L-lactate (n = 3).

Data are presented as mean ± standard error of the mean (SEM) (A, C, E). Statistics: unpaired Students t-test *p < 0.05, **p < 0.01.

alone is not sufficient to elicit the effect. We thus hypothesized that the pro-proliferative effect of L-lactate is either independent of HCAR1 or HCAR1 activation is relevant only together with the substrate effects of L-lactate. To address this, we generated NPCs with deletion of *Hcar1* (HCAR1-KO) using CRISPR-Cas9 technology (Figure 6B) and assessed proliferation using an EdU/DAPI-based cell cycle analysis (Figure S2). We found that HCAR1-KO NPCs responded similar to control cells (LacZ) to L-lactate treatment in that the relative amount of cells in S-phase was increased compared to untreated NPCs (LacZ: one-way ANOVA [$F(2,9) = 12.51$, $p = 0.0025$], $n = 4$; Dunnett's *post hoc*, 20 mM $p = 0.0016$; HCAR1: one-way ANOVA [$F(2,6) = 5.871$, $p = 0.0385$], $n = 3$; Dunnett's *post hoc*, 20 mM $p = 0.026$; Figures 6C and 6D). Taken together, these data show that HCAR1 is not crucial for the L-lactate-induced increase in NPC proliferation.

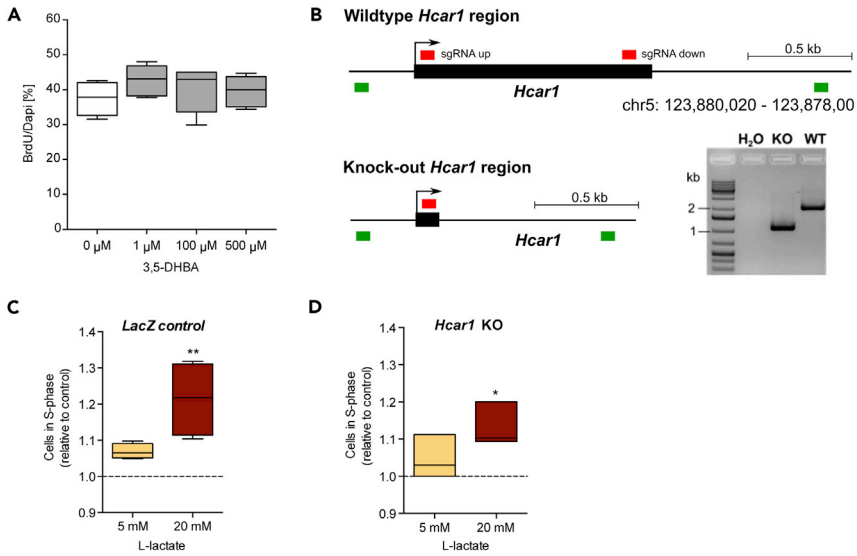

Figure 6. Knockout of *Hcar1* does not deplete the pro-proliferative effect of L-lactate

(A) Percentages of BrdU-positive cells after treatment with HCAR1 agonist 3,5-DHBA (n = 5).

(B) Schematic of CRISPR-Cas9 strategy for knockout of Hcar1, sgRNAs are highlighted in red, primers used for genotyping are highlighted in green. Agarose gel of PCR products using genotyping primers validates *Hcar1*-KO efficacy.

(C) Relative number of L-lactate treated NPCs in S-phase (at 2.5 hr after EdU incorporation) in control (LacZ) cells (n = 4).

(D) Relative number of L-lactate-treated HCAR1-KO cells in S-phase (at 2.5 hr after EdU incorporation; n = 3).

Statistics: one-way ANOVA with Dunnett's *post hoc*; *p < 0.05, **p < 0.01.

L-lactate induces ERK1/2 and Akt signaling

In order to further understand the mechanism behind the L-lactate-induced increase in proliferative potential, we next investigated whether L-lactate would induce the phosphorylation of ERK1/2 or Akt in hippocampal NPCs, two pathways associated with regulation of proliferation. To that end, we analyzed phosphorylation of ERK1/2 (p44/42 MAPK, Thr202/Tyr204) in a time-dependent manner (Figure 7A) and found that L-lactate (20 mM) indeed induced a transient, statistically significant (two-way ANOVA [$F(1,50) = 6.28$, $p = 0.015$]; n = 6; Fisher's LSD *post hoc*; Figure 7B) increase in phosphorylation of ERK1/2 after 1 hr ($p = 0.014$) and 3 hr ($p = 0.045$). Furthermore, we investigated the PI3K/Akt signaling pathway, as it plays a central role in the regulation of cell proliferation. We thus examined how L-lactate affected the phosphorylation of Akt (Ser473) in hippocampal NPCs and observed—similar to ERK1/2—a time-dependent significant (two-way ANOVA [$F(1,50) = 5.271$, $p = 0.026$]; n = 6; Fisher's LSD *post hoc*; Figure 7C) increase of Akt activation after 3 hr ($p = 0.008$) of L-lactate treatment. Moreover, through inhibition of PI3K with LY294002 (50 µg), we further demonstrated that the increase in Akt phosphorylation was dependent on PI3K activation as no difference in phosphorylation levels was found between control and L-lactate treated cells after inhibitor treatment (n = 3; Figures 7D and 7E). These data suggest that L-lactate may act as a signaling molecule independent of HCAR1 by activating at least two signaling pathways known to stimulate proliferation.

DISCUSSION

In this study, we have shown that L-lactate, a rather ubiquitous intermediate of cellular energy metabolism, elicits a pro-proliferative effect on adult hippocampal precursor cells *in vitro*. Importantly, this effect was dependent on transporter-dependent trafficking of L-lactate while HCAR1-mediated signaling was not crucial. Our results suggest an intricate interaction between energy metabolism and metabolite-induced signaling in NPCs, as it has been suggested for the regulation of cellular state, function, and behavior in other contexts (Rafalski et al., 2012; Husted et al., 2017; Wang and Lei 2018). Although the conclusions of the present study are limited to our *in vitro* findings and need to be further validated *in vivo*, they imply that exogenous L-lactate might act as a mediator of cellular homeostasis and activity-dependent plasticity in adult hippocampal neurogenesis *in vivo*.

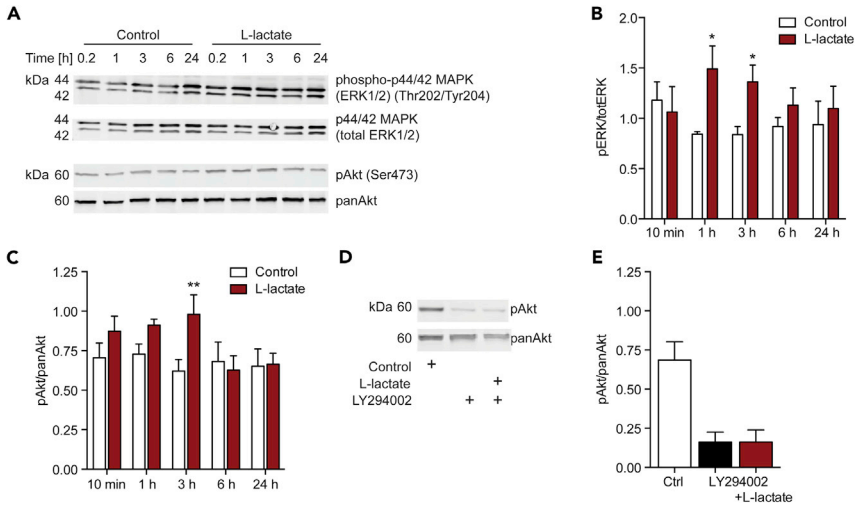

Figure 7. L-lactate induces phosphorylation of ERK1/2 and Akt

(A) Representative Western blots of phosphor-p44/42 MAPK (pERK1/2), p44/42 MAPK (totERK1/2), pAkt, and panAkt, following stimulation with L-lactate (0 or 20 mM).

(B) Ratios of pERK/totERK after stimulation with L-lactate for the indicated time (n = 6).

(C) Ratios of pAkt/panAkt after stimulation with L-lactate for the indicated time (n = 6).

(D) Representative Western blot of pAkt and panAkt upon treatment with PI3K inhibitor LY294002.

(E) Ratios of pAkt/panAkt following treatment with LY294002 (n = 3).

Bar graphs represent mean ± standard error of the mean (SEM).

Statistics: two-way ANOVA with Fisher's LSD *post hoc*; *p < 0.05, **p < 0.01.

L-lactate augments the proliferative potential of hippocampal NPCs

While energy metabolism emerged as a key player regulating cellular homeostasis (Folmes et al., 2011; Knobloch et al., 2013; Ito and Suda 2014; Homem et al., 2015), it is still unclear whether the availability of metabolites can influence specific processes, such as stem cell activation, proliferation, or lineage progression. In addition, there is evidence that changes in energy metabolism not only accompany but also precede the activation of quiescent stem cells, thereby potentially priming neural stem cells to be responsive to other stimuli that further the transition to proliferation (Llorens-Bobadilla et al., 2015; Shin et al., 2015). However, in our model of quiescent NPCs (BMP4), L-lactate supplementation did not stimulate proliferation. Interestingly, BMP4-treated NPCs showed increased expression of the L-lactate exporters *Slc16a3* (MCT4) and *Slc16a1* (MCT1) consistent with the glycolytic profile of quiescent cells (Maurer et al., 2006; Candelario et al., 2013; Shin et al., 2015). We therefore conclude that L-lactate cannot trigger a change in the functional and metabolic state of BMP4-treated NPCs. We did, however, find that L-lactate increased the proliferation and the percentage of dividing NPCs and that the increase in proliferation was associated with a decrease in generation time. A recent study conducted on postnatal NPCs corroborates our finding that L-lactate augments NPC proliferation by showing that lactate promotes cellular self-renewal *in vitro* (Álvarez et al., 2016). Moreover, reduction of cell cycle length has been described as a feature of activated neural stem cells that, following rapid division, give rise to more committed progenitors (Encinas et al., 2011; Brandt et al., 2012). Indeed, it becomes increasingly evident that NPCs are not a homogeneous but a rather heterogeneous population with distinct subtypes of latent NPCs that respond selectively to diverse of stimuli (Walker et al. 2008, 2016; Lugert et al., 2010; Encinas et al., 2011; Jhaveri et al., 2015). As our *in vitro* NPCs represent a mixture of NPCs of varying early developmental stages, it is likely that L-lactate could induce rapid proliferation in a subpopulation of latent NPCs accounting for the increase in dividing cells, the reduction in cell cycle length, and the increased number of neurospheres. Conversely, cell cycle shortening is also a parameter associated with commitment of neural precursors to the neuronal lineage (Brandt et al., 2012). In addition, transition from aerobic glycolysis to oxidative phosphorylation was shown to be critical for neuronal differentiation (Zheng et al., 2016). We therefore hypothesized that L-lactate would promote neuronal fate determination during differentiation but did not find a significant effect in both neurosphere and adherent NPCs. However, one major caveat of NPCs *in vitro* is the lack of developmental stages and incomplete differentiation besides the absence of inputs from the cellular environment. Consequently, we here do not exclude that L-lactate could promote neuronal survival and differentiation *in vivo*.

Role of L-lactate in energy metabolism of NPCs

Controlling the cellular energy metabolism is critically important for the activity of adult precursor cells and during cellular reprogramming. Historically, high rates of proliferation have been considered to be associated with high rates of glycolytic flux regardless of oxygen availability —a phenomenon known as the Warburg effect (Warburg 1925; Vander Heiden et al., 2009). Interestingly, proliferating stem or progenitor cells are often attributed to exhibit Warburg-like metabolic features due to their high glucose metabolism (Vander Heiden et al., 2009; Kim et al., 2015).

By assessing the glycolytic flux, we found, however, that in our NPCs, glycolysis was significantly decreased after L-lactate treatment, which argues against the idea that the increase in proliferation was associated with Warburg-like metabolic reprogramming. Indeed, reduced glycolysis in response to exogenous L-lactate availability has been reported before, indicating a negative feedback mechanism (Sotelo-Hitschfeld et al., 2012) or altered Phosphofructokinase (PFK) activity (Leite et al. 2007, 2011) as responsible for the reduction. Intriguingly, we found that while glycolytic flux was reduced, consumption of glucose was not different between treated and untreated NPCs. Moreover, exposure to L-lactate increased G6PD activity, the key enzyme of the PPP. This finding is interesting as one of the proposed roles of glucose consumption in dividing cells is linked not only to ATP production but also to the PPP. The PPP generates NADPH, regulates redox homeostasis, and enables biosynthesis of lipids and nucleotides, thereby promoting cell growth and proliferation (Tian et al., 1998; Jiang et al., 2011; Xu et al., 2016). Since G6PD is the rate limiting enzyme of the PPP, it acts as a gatekeeper and thus reflects activity of the oxidative branch of the pathway. Consequently, we propose that exposure to L-lactate leads to increased direction of glucose toward the PPP in adult NPCs.

Based on the ANLSH and the observation that energy production of proliferating NPCs depended not only on glycolysis but also on mitochondrial respiration (Llorens-Bobadilla et al., 2015; Beckervordersandforth et al., 2017), we suspected that concomitantly to an increase in proliferation, the availability of L-lactate might lead to increased oxidative phosphorylation. Under our experimental conditions, however, we did not detect any change in mitochondrial respiration suggesting no causal relationship between L-lactate-dependent ATP production and the increase in NPC proliferation.

MCT-mediated transport of L-lactate is required for its pro-proliferative effect

Entry of L-lactate into neurons and increased NADH levels have previously been described as a mechanism through which L-lactate induces NMDA receptor-mediated immediate-early gene expression (Yang et al., 2014). In addition, knockdown of MCT2 in the hippocampus resulted in impairments in long-term memory formation (Suzuki et al., 2011) and inhibition of MCT2 depleted the pro-survival effect of L-lactate on newly generated neurons during adult neurogenesis (Lev-Vachnish et al., 2019). These studies describe an important functional role for L-lactate transport. We corroborated the importance of L-lactate trafficking by showing that complete inhibition of MCT2 (100%) and partial inhibition of MCT1 (approx. 12.5%) abolished the effect of L-lactate on NPC proliferation. This suggests that while in proliferating NPCs L-lactate might not contribute to mitochondrial respiration, its transport, conversion, and subsequent use as substrate in metabolic pathways might still be essential. Here, it is tempting to speculate that the uptake of L-lactate by proliferating NPCs is associated with *de novo* lipogenesis with L-lactate serving as a carbon source. *De novo* lipogenesis is a key factor in facilitating NPC proliferation (Knobloch et al., 2013). Interestingly, lipogenesis relies on the availability of NADPH, which is provided through the PPP (Jin et al., 2018). Our finding that G6PD activity, here a proxy for PPP action, was increased further supports the notion that *de novo* lipogenesis fueled by L-lactate might contribute to the increased proliferation of NPCs.

L-lactate stimulates ERK1/2 and PI3K/Akt signaling

While we demonstrated that HCAR1 activation was not crucial to increase proliferation, we still observed a transient increase in the phosphorylation level of both ERK1/2 and Akt following L-lactate treatment. However, the mechanisms behind these observations still need to be investigated in detail but they show exemplarily that the presence of L-lactate affects cell signaling. Although deletion of *Hcar1* did not abolish the pro-proliferative effect of L-lactate, based on the current data, we cannot exclude that the increase in ERK1/2 and Akt phosphorylation could be caused by L-lactate-stimulated activation of HCAR1. Alternatively, these signaling pathways could be induced through HCAR1-independent mechanisms. Accordingly, one study suggests the existence of a yet unidentified excitatory GPCR (Tang et al., 2014) while other studies describe indirect signaling properties of L-lactate following its uptake by the cell

(Parsons and Hirasawa, 2010; Ruan and Kazlauskas 2013; Yang et al., 2014). Indeed, activation of ERK1/2 signaling was associated with an increase in the NADH:NAD^+ ratio caused by the conversion of L-lactate to pyruvate, thereby implicating L-lactate as an indirect signaling molecule (Yang et al., 2014). As ERK1 signaling is associated with the regulation of cell proliferation, differentiation, and apoptosis (Zhang and Liu 2002; Yanamadala et al., 2009), it seems likely that its increased activity following L-lactate treatment adds to its pro-proliferative effect. However, this causality needs to be determined in future experiments. Similar to ERK1/2, indirect signaling properties of L-lactate regarding the activation of Akt were also described as L-lactate was shown to stimulate phosphorylation of Akt in endothelial cells by promoting the activation of multiple receptor tyrosine kinases (Ruan and Kazlauskas 2013). Interestingly, PI3K/Akt signaling is a known regulator of glucose metabolism and was shown to mediate proliferation (Singh et al., 2008; Düvel et al., 2010; Mitsuishi et al., 2012; Tsouko et al., 2014; Ricoult et al., 2016). Indeed, the most prominent downstream target of the PI3K/Akt signaling pathway, rapamycin, was shown to be involved in the regulation of G6PD, thereby influencing cell proliferation (Düvel et al., 2010; Tsouko et al., 2014). We therefore propose that L-lactate-mediated stimulation of PI3K/Akt might regulate the observed increase in G6PD activity. This link and the exact signaling properties and mechanisms of L-lactate need to be shown conclusively but likely contribute to the pro-proliferative effect of L-lactate on adult NPCs. Still, by demonstrating in an exemplary nature that the presence of L-lactate does have an effect on the activity of two signaling pathways commonly associated with cell proliferation and survival, we emphasize that L-lactate, as a signaling molecule, should be the focus of further studies.

Role of L-lactate for adult hippocampal neurogenesis

Adult hippocampal neurogenesis provides a unique form of flexibility and adaptability in response to environmental inputs. Lifestyle factors such as physical activity, environmental enrichment, and spatial learning are positively associated with the proliferation and/or survival potential of NPCs and newly generated neurons (Kempermann et al., 1997; van Praag et al., 1999a, 1999b; Kronenberg et al., 2003; Dupret et al., 2007). Interestingly, both exercise effects and learning performance have been linked to L-lactate availability (Ferreira et al., 2007; Suzuki et al., 2011; Matsui et al., 2017; El Hayek et al., 2019). This suggests a potential role for L-lactate in mediating behavioral effects on plasticity. In this study, we used L-lactate as a proxy for behavioral activity and considered its effects on NPCs *in vitro*. We found that L-lactate significantly increased proliferation of adult hippocampal NPCs, while proliferation of NPCs from the SVZ was not altered. This parallels our previous observation that exercise does not increase proliferation of NPCs in the SVZ *in vivo* (Brown et al., 2003). The selective responsiveness of hippocampal NPCs to L-lactate *in vitro* implies that availability of this metabolite in response to behavioral activity might contribute to adaptive processes of adult neurogenesis. Indeed, two recent studies using different paradigms involving the systemic administration of L-lactate showed that in one case L-lactate increased the survival of newly generated neurons but did not improve spatial learning (Lev-Vachnish et al., 2019) and in the other showed enhanced spatial learning performance and hippocampal expression of *Bdnf* (El Hayek et al., 2019). Both findings were attributed to the substrate properties of L-lactate as the effects on neurogenesis and learning could not be mimicked by 3,5-DHBA and were abolished by inhibition of MCTs (El Hayek et al., 2019; Lev-Vachnish et al., 2019). Our study also showed that the effect of L-lactate was dependent on MCT-mediated transport and further proposed that L-lactate might serve as a carbon source for *de novo* lipogenesis. Another recent study emphasized that lactate homeostasis plays an important role in controlling adult hippocampal neurogenesis (Wang et al., 2019). In contrast to the studies discussed above, the authors here describe that increased lactate levels have a negative effect on adult hippocampal neurogenesis and hippocampus-dependent learning as lactate treatment was associated with a reduced stem cell pool and terminal differentiation. However, the study did corroborate our finding that L-lactate stimulates proliferation as the number of BrdU-positive cells was increased following lactate injection (Wang et al., 2019). Although these studies (El Hayek et al., 2019; Lev-Vachnish et al., 2019; Wang et al., 2019) seem at odds regarding the effect of lactate on adult neurogenesis *in vivo*, they illustrate that lactate concentration matters and that the sensitivity as well as the response of different cell types to lactate varies (Scandella and Knobloch, 2019). This emphasizes that the metabolic microenvironment and finely tuned lactate homeostasis are important regulators of hippocampal neurogenesis that should be further explored.

It remains a major challenge to uncover how lifestyle factors enable the potentiation of brain plasticity and cognitive function through the activation of adult hippocampal neurogenesis. Here, we propose that through the interaction of its signaling and substrate properties, L-lactate acts as a trigger for plasticity in the context of adult hippocampal neurogenesis. We suggest that L-lactate contributes to the

homeostatic adaption of cellular processes required for adaptive changes in the production of new neurons in the DG in response to activation on the behavioral level.

LIMITATIONS OF THE STUDY

Our study reveals an interesting and novel role of L-lactate in neural stem cell biology but currently remains limited to our *in vitro* approach. Placing the current findings into the *in vivo* context poses a considerable additional experimental challenge that is difficult to address due to the ubiquity of lactate in the body. At this time, we also could not yet relate our findings to the interesting question of how redox state and energy metabolism in general are involved in the control of stem cell activity, where lactate is likely to play an interesting role (Adusumilli et al., 2020). Our demonstration of lactate effects on ERK1/2 and PI3K/Akt does not yet constitute proof that lactate affects proliferation through this pathway (alone). Manipulations of ERK1/2 and PI3K/Akt would be necessary to lead that proof. As a small additional caveat, we have not been able to fulfill a reasonable reviewer's request to demonstrate the successful HCAR1 knockdown at the protein level because we could not maintain our cell cultures during the corona lockdowns in 2020 and early 2021. Given the nature of the CRISPR approach and the demonstration at the PCR level, however, we are confident of the successful knockdown.

RESOURCE AVAILABILITY

Lead contact

Further information and requests should be directed to and will be fulfilled by the lead contact, Gerd Kempermann (gerd.kempermann@dzne.de)

Material availability

This study did not generate new unique reagents.

Data code availability

The published article includes all data sets generated or analyzed during this study. The code supporting the current study (tracking data) has not been deposited in a public repository yet because they are in the process of being published in a separate study.

METHODS

All methods can be found in the accompanying Transparent Methods supplemental file.

SUPPLEMENTAL INFORMATION

Supplemental Information can be found online at https://doi.org/10.1016/j.isci.2021.102126.

ACKNOWLEDGMENTS

Images were acquired using equipment of the imaging platform at the DZNE Dresden with the support of Silke White. Seahorse Analyzer experiments were performed at the MPI-CBG Dresden with the support of Rico Barsacchi. The research was funded by BMBF through the EnergI consortium (01GQ1421B) and by the Virtual Institute (VH-VI-510) of the Helmholtz Association (HGF).

AUTHOR CONTRIBUTION

Conceptualization, A.P. and G.K.; Methodology, A.P., S.N.B., O.L., and S.Z.; Investigation, A.P., S.N.B., O.L., and S.Z.; Writing – original draft, A.P.; Writing – review and editing, G.K., A.P., A.R., O.L., S.Z., and S.N.B.; Funding acquisition and supervision, G.K. and A.R.

DECLARATION OF INTEREST

The authors declare no competing interests.

Received: September 16, 2019
Revised: June 5, 2020
Accepted: January 27, 2021
Published: February 19, 2021

REFERENCES

Adusumilli, V.S., Walker, T.L., Overall, R.W., Klatt, G.M., Zeidan, S.A., Zocher, S., Kirova, D.G., Ntitsias, K., Fischer, T.J., Sykes, A.M., et al. (2020). ROS dynamics delineate functional states of hippocampal neural stem cells and link to their activity-dependent exit from quiescence. Cell Stem Cell *2*, 300–314.

Álvarez, Z., Hyroššová, P., Perales, J.C., and Alcántara, S. (2016). Neuronal progenitor maintenance requires lactate metabolism and PEPCK-M-directed cataplerosis. Cereb. Cortex *26*, 1046–1058.

Babu, H., Cheung, G., Kettenmann, H., Palmer, T.D., and Kempermann, G. (2007). Enriched monolayer precursor cell cultures from micro-dissected adult mouse dentate gyrus yield functional granule cell-like neurons. PLoS One *2*, e388.

Beckervordersandforth, R., Ebert, B., Schäffner, I., Moss, J., Fiebig, C., Shin, J., Moore, D.L., Ghosh, L., Trinchero, M.F., Stockburger, C., et al. (2017). Role of mitochondrial metabolism in the control of early lineage progression and aging phenotypes in adult hippocampal neurogenesis. Neuron *93*, 560–573.

Bélanger, M., Allaman, I., and Magistretti, P.J. (2011). Brain energy metabolism: focus on Astrocyte-neuron metabolic cooperation. Cell Metab. *14*, 724–738.

Bergersen, L.H. (2015). Lactate transport and signaling in the brain: potential therapeutic targets and roles in body–brain interaction. J. Cereb. Blood Flow Metab. *35*, 176–185.

Bouzier-Sore, A.K., Voisin, P., Bouchaud, V., Bezancon, E., Franconi, J.M., and Pellerin, L. (2006). Competition between glucose and lactate as oxidative energy substrates in both neurons and astrocytes: a comparative NMR study. Eur. J. Neurosci. *24*, 1687–1694.

Bozzo, L., Puyal, J., and Chatton, J.-Y. (2013). Lactate modulates the activity of primary cortical neurons through a receptor-mediated pathway. PLoS One *8*, e71721.

Brandt, M.D., Hübner, M., and Storch, A. (2012). Adult hippocampal precursor cells shorten S-phase and total cell cycle length during neuronal differentiation. Stem Cells *30*, 2843–2847.

Bröer, S., Bröer, A., Schneider, H.-P., Stegen, C., Halestrap, A.P., and Deitmer, J.W. (1999). Characterization of the high-affinity monocarboxylate transporter MCT2 in Xenopus laevis oocytes. Biochem. J. *341*, 529–535.

Brooks, G.A. (2009). Cell-cell and intracellular lactate shuttles. J. Physiol. *587*, 5591–5600.

Brown, J., Cooper-Kuhn, C.M., Kempermann, G., van Praag, H., Winkler, J., Gage, F.H., and Kuhn, H.G. (2003). Enriched environment and physical activity stimulate hippocampal but not olfactory bulb neurogenesis. Eur. J. Neurosci. *17*, 2042–2046.

Cai, T.Q., Ren, N., Jin, L., Cheng, K., Kash, S., Chen, R., Wright, S.D., Taggart, A.K.P., and Waters, M.G. (2008). Role of GPR81 in lactate-mediated reduction of adipose lipolysis. Biochem. Biophys. Res. Commun. *377*, 987–991.

Candelario, K.M., Shuttleworth, C.W., and Cunningham, L.A. (2013). Neural stem/progenitor cells display a low requirement for oxidative metabolism independent of hypoxia inducible factor-1alpha expression. J. Neurochem. *125*, 420–429.

Cavallucci, V., Fidaleo, M., and Pani, G. (2016). Neural stem cells and nutrients : poised between quiescence and exhaustion. Trends Endocrinol. Metab. *27*, 756–769.

Dupret, D., Fabre, A., Döbrössy, M.D., Panatier, A., Rodríguez, J.J., Lamarque, S., Lemaire, V., Oliet, S.H.R., Piazza, P.V., and Abrous, D.N. (2007). Spatial learning depends on both the addition and removal of new hippocampal neurons. PLoS Biol. *5*, 1683–1694.

Düvel, K., Yecies, J.L., Menon, S., Raman, P., Lipovsky, A.I., Souza, A.L., Triantafellow, E., Ma, Q., Gorski, R., Cleaver, S., et al. (2010). Activation of a metabolic gene regulatory network downstream of mTOR complex 1. Mol. Cell *39*, 171–183.

El Hayek, L., Khalifeh, M., Zibara, V., Abi Assaad, R., Emmanuel, N., Karnib, N., El-Ghandour, R., Nasrallah, P., Bilen, M., Ibrahim, P., et al. (2019). Lactate mediates the effects of exercise on learning and memory through SIRT1-dependent activation of hippocampal brain-derived neurotrophic factor (BDNF). J. Neurosci. *39*, 2369–2382.

Encinas, J.M., Michurina, T.V., Peunova, N., Park, J.-H., Tordo, J., Peterson, D.A., Fishell, G., Koulakov, A., and Enikolopov, G. (2011). Division-coupled astrocytic differentiation and age-related depletion of neural stem cells in the adult hippocampus. Cell Stem Cell *8*, 566–579.

Erlichman, J.S., Hewitt, A., Damon, T.L., Hart, M., Kurascz, J., Li, A., and Leiter, J.C. (2009). Inhibition of monocarboxylate transporter 2 in the retrotrapezoid nucleus in rats – a test of the astrocyte-neuron lactate-shuttle hypothesis. J. Neurosci. *28*, 4888–4896.

Ferreira, J.C.B., Rolim, N.P.L., Bartholomeu, J.B., Gobatto, C.A., Kokubun, E., and Brum, P.C. (2007). Maximal lactate steady state in running mice: effect of exercise training. Clin. Exp. Pharmacol. Physiol. *34*, 760–765.

Folmes, C.D.L., Nelson, T.J., Martinez-Fernandez, A., Arrell, D.K., Lindor, J.Z., Dzeja, P.P., Ikeda, Y., Perez-Terzic, C., and Terzic, A. (2011). Somatic oxidative bioenergetics transitions into pluripotency-dependent glycolysis to facilitate nuclear reprogramming. Cell Metab. *14*, 264–271.

Garthe, A., Roeder, I., and Kempermann, G. (2016). Mice in an enriched environment learn more flexibly because of adult hippocampal neurogenesis. Hippocampus *26*, 261–271.

Gordon, G.R.J., Choi, H.B., Rungta, R.L., Ellis-Davies, G.C.R., and MacVicar, B.A. (2008). Brain metabolism dictates the polarity of astrocyte control over arterioles. Nature *456*, 745–750.

Guilak, F., Cohen, D.M., Estes, B.T., Gimble, J.M., Liedtke, W., and Chen, C.S. (2009). Control of stem cell fate by physical interactions with the extracellular matrix. Cell Stem Cell *5*, 17–26.

Hashimoto, T., Hussien, R., Cho, H.S., Kaufer, D., and Brooks, G.A. (2008). Evidence for the mitochondrial lactate oxidation complex in rat neurons: demonstration of an essential component of brain lactate shuttles. PLoS One *3*, e2915.

Homem, C.C.F., Repic, M., and Knoblich, J.A. (2015). Proliferation control in neural stem and progenitor cells. Nat. Rev. Neurosci. *16*, 647–659.

Husted, A.S., Trauelsen, M., Rudenko, O., Hjorth, S.A., and Schwartz, T.W. (2017). GPCR-mediated signaling of metabolites. Cell Metab. *25*, 777–796.

Ito, K., and Suda, T. (2014). Metabolic requirements for the maintenance of self-renewing stem cells. Nat. Rev. Mol. Cell Biol. *15*, 243–256.

Jhaveri, D.J., O'Keeffe, I., Robinson, G.J., Zhao, Q.-Y., Zhang, Z.H., Nink, V., Narayanan, R.K., Osborne, G.W., Wray, N.R., and Bartlett, P.F. (2015). Purification of neural precursor cells reveals the presence of distinct, stimulus-specific subpopulations of quiescent precursors in the adult mouse hippocampus. J. Neurosci. *35*, 8132–8144.

Jiang, P., Du, W., Wang, X., Mancuso, A., Gao, X., Wu, M., and Yang, X. (2011). p53 regulates biosynthesis through direct inactivation of glucose-6-phosphate dehydrogenase. Nat. Cell Biol *13*, 310–316.

Jin, E.S., Lee, M.H., Murphy, R.E., and Malloy, C.R. (2018). Pentose phosphate pathway activity parallels lipogenesis but not antioxidant processes in rat liver. Am. J. Physiol. Metab. *314*, E543–E551.

Kempermann, G. (2011). Seven principles in the regulation of adult neurogenesis. Eur. J. Neurosci. *33*, 1018–1024.

Kempermann, G. (2015). Activity dependency and aging in the regulation of adult neurogenesis. Cold Spring Harb. Perspect. Biol. *7*, a018929.

Kempermann, G., Jessberger, S., Steiner, B., and Kronenberg, G. (2004). Milestones of neuronal development in the adult hippocampus. Trends Neurosci. *27*, 447–452.

Kempermann, G., Kuhn, H.G., and Gage, F.H. (1997). More hippocampal neurons in adult mice living in an enriched environment. Nature *386*, 493–495.

Kim, D.Y., Rhee, I., and Paik, J. (2015). Metabolic circuits in neural stem cells. Cell Mol. Life Sci. *71*, 4221–4241.

Knobloch, M., Braun, S.M.G., Zurkirchen, L., von Schoultz, C., Zamboni, N., Araúzo-Bravo, M.J., Kovacs, W.J., Karalay, O., Suter, U., Machado, R.A.C., et al. (2013). Metabolic control of adult neural stem cell activity by Fasn-dependent lipogenesis. Nature *493*, 226–230.

Kronenberg, G., Reuter, K., Steiner, B., Brandt, M.D., Jessberger, S., Yamaguchi, M., and Kempermann, G. (2003). Subpopulations of proliferating cells of the adult hippocampus respond differently to physiologic neurogenic stimuli. J. Comp. Neurol. *467*, 455–463.

Lafenêtre, P., Leske, O., Ma-Högemeie, Z., Haghikia, A., Bichler, Z., Whale, P., and Heumann, R. (2010). Exercise can rescue recognition memory impairment in a model with reduced adult hippocampal neurogenesis. Front. Behav. Neurosci. *3*, 34.

Lauritzen, K.H., Morland, C., Puchades, M., Holm-Hansen, S., Hagelin, E.M., Lauritzen, F., Attramadal, H., Storm-Mathisen, J., Gjedde, A., and Bergersen, L.H. (2014). Lactate receptor sites link neurotransmission, neurovascular coupling, and brain energy metabolism. Cereb. Cortex *24*, 2784–2795.

Lee, D.K., Nguyen, T., Lynch, K.R., Cheng, R., Vanti, W.B., Arkhitko, O., Lewis, T., Evans, J.F., George, S.R., and O'Dowd, B.F. (2001). Discovery and mapping of ten novel G protein-coupled receptor genes. Gene *275*, 83–91.

Leite, T.C., Coelho, R.G., Da Silva, D., Coelho, W.S., Marinho-Carvalho, M.M., and Sola-Penna, M. (2011). Lactate downregulates the glycolytic enzymes hexokinase and phosphofructokinase in diverse tissues from mice. FEBS Lett. *585*, 92–98.

Leite, T.C., Sola-Penna, M., Guimarães Coelho, R., Zancan, P., and Da Silva, D. (2007). Lactate favours the dissociation of skeletal muscle 6-phosphofructo-1-kinase tetramers down-regulating the enzyme and muscle glycolysis. Biochem. J. *408*, 123–130.

Leiter, O., Seidemann, S., Overall, R.W., Ramasz, B., Rund, N., Schallenberg, S., Grinenko, T., Wielockx, B., Kempermann, G., and Walker, T.L. (2019). Exercise-induced activated platelets increase adult hippocampal precursor proliferation and promote neuronal differentiation. Stem Cell Rep. *12*, 667–679.

Lev-Vachnish, Y., Cadury, S., Rotter-Maskowitz, A., Feldman, N., Roichman, A., Illouz, T., Varvak, A., Nicola, R., Madar, R., and Okun, E. (2019). L-lactate promotes adult hippocampal neurogenesis. Front. Neurosci. *13*, 1–13.

Liu, C., Wu, J., Zhu, J., Kuei, C., Yu, J., Shelton, J., Sutton, S.W., Li, X., Su, J.Y., Mirzadegan, T., et al. (2009). Lactate inhibits lipolysis in fat cells through activation of an orphan G-protein-coupled receptor, GPR81. J. Biol. Chem. *284*, 2811–2822.

Llorens-Bobadilla, E., Zhao, S., Baser, A., Saiz-Castro, G., Zwadlo, K., and Martin-Villalba, A. (2015). Single-cell transcriptomics reveals a population of dormant neural stem cells that become activated upon brain injury. Cell Stem Cell *17*, 1–12.

Lugert, S., Basak, O., Knuckles, P., Haussler, U., Fabel, K., Götz, M., Haas, C.A., Kempermann, G., Taylor, V., and Giachino, C. (2010). Quiescent and active hippocampal neural stem cells with distinct morphologies respond selectively to physiological and pathological stimuli and aging. Cell Stem Cell *6*, 445–456.

Mächler, P., Wyss, M.T., Elsayed, M., Stobart, J., Gutierrez, R., von Faber-Castell, A., Kaelin, V., Zuend, M., San Martin, A., Romero-Gómez, I., et al. (2016). In vivo evidence for a lactate gradient from astrocytes to neurons. Cell Metab. *23*, 94–102.

Martynoga, B., Mateo, J.L., Zhou, B., Andersen, J., Achimastou, A., Urbán, N., van den Berg, D., Georgopoulou, D., Hadjur, S., Wittbrodt, J., et al. (2013). Epigenomic enhancer annotation reveals a key role for NFIX in neural stem cell quiescence. Genes Dev. *27*, 1769–1786.

Matsui, T., Omuro, H., Liu, Y., Soya, M., Shima, T., McEwen, B.S., and Soya, H. (2017). Astrocytic glycogen-derived lactate fuels the brain during exhaustive exercise to maintain endurance capacity. Proc. Natl. Acad. Sci. *114*, 6358–6363.

Maurer, M.H., Geomor, H.K., Bürgers, H.F., Schelshorn, D.W., and Kuschinsky, W. (2006). Adult neural stem cells express glucose transporters GLUT1 and GLUT3 and regulate GLUT3 expression. FEBS Lett. *580*, 4430–4434.

Mitsuishi, Y., Taguchi, K., Kawatani, Y., Shibata, T., Nukiwa, T., Aburatani, H., Yamamoto, M., and Motohashi, H. (2012). Nrf2 redirects glucose and glutamine into anabolic pathways in metabolic reprogramming. Cancer Cell *22*, 66–79.

Morland, C., Andersson, K.A., Haugen, Ø.P., Hadzic, A., Kleppa, L., Gille, A., Rinholm, J.E., Palibrk, V., Diget, E.H., Kennedy, L.H., et al. (2017). Exercise induces cerebral VEGF and angiogenesis via the lactate receptor HCAR1. Nat. Commun. *8*, 15557.

Palmer, T.D., Ray, J., and Gage, F.H. (1995). FGF-2-responsive neuronal progenitors reside in proliferative and quiescent regions of the adult rodent brain. Mol. Cell Neurosci. *6*, 474–486.

Parsons, M.P., and Hirasawa, M. (2010). ATP-sensitive potassium channel-mediated lactate effect on orexin neurons: Implications for brain energetics during arousal. J. Neurosci. *30*, 8061–8070.

Pellerin, L., Halestrap, A.P., and Pierre, K. (2005). Cellular and subcellular distribution of monocarboxylate transporters in cultured brain cells and in the adult brain. J. Neurosci. Res. *79*, 55–64.

Pellerin, L., and Magistretti, P.J. (1994). Glutamate uptake into astrocytes stimulates aerobic glycolysis: a mechanism coupling neuronal activity to glucose utilization. Proc. Natl. Acad. Sci. *91*, 10625–10629.

Rafalski, V.A., Mancini, E., and Brunet, A. (2012). Energy metabolism and energy-sensing pathways in mammalian embryonic and adult stem cell fate. J. Cell Sci. *125*, 5597–5608.

Rafiki, A., Boulland, J.L., Halestrap, A.P., Ottersen, O.P., and Bergersen, L. (2003). Highly differential expression of the monocarboxylate transporters MCT2 and MCT4 in the developing rat brain. Neuroscience *122*, 677–688.

Ray, J., Raymon, H.K., and Gage, F.H. (1995). Generation and culturing of precursor cells and neuroblasts from embryonic and adult central nervous system. Methods Enzymol. *254*, 20–37.

Reynolds, B.A., and Weiss, S. (1992). Generation of neurons and astrocytes from isolated cells of the adult mammalian central nervous system. Science *255*, 1707–1710.

Ricoult, S.J.H., Yecies, J.L., Ben-Sahra, I., and Manning, B.D. (2016). Oncogenic PI3K and K-Ras stimulate de novo lipid synthesis through mTORC1 and SREBP. Oncogene *35*, 1250–1260.

Rouach, N., Koulakoff, A., Abudara, V., Willecke, K., and Giaume, C. (2008). Astroglial metabolic networks sustain hippocampal synaptic transmission. Science *322*, 1551–1555.

Ruan, G.-X., and Kazlauskas, A. (2013). Lactate engages receptor tyrosine kinases Axl, Tie2, and vascular endothelial growth factor receptor 2 to activate phosphoinositide 3-kinase/AKT and promote angiogenesis. J. Biol. Chem. *288*, 21161–21172.

Scadden, D.T. (2006). The stem-cell niche as an entity of action. Nature *441*, 1075–1079.

Scandella, V., and Knobloch, M. (2019). Sensing the Environment: Extracellular Lactate Levels Control Adult Neurogenesis. Cell Stem Cell *25*, 729–731.

Schurr, A., West, C.A., and Rigor, B.M. (1988). Lactate-supported synaptic function in the rat hippocampal slice preparation. Sci. Sci. *240*, 1326–1328.

Shin, J., Berg, D.A., Zhu, Y., Shin, J.Y., Bonaguidi, M.A., Enikolopov, G., Nauen, D.W., Christian, K.M., Ming, G., and Song, H. (2015). Single-cell RNA-seq with waterfall reveals molecular cascades underlying adult neurogenesis. Cell Stem Cell *17*, 360–372.

Singh, A., Boldin-Adamsky, S., Thimmulappa, R.K., Rath, S.K., Ashush, H., Coulter, J., Blackford, A., Goodman, S.N., Bunz, F., Watson, W.H., et al. (2008). RNAi-mediated silencing of nuclear factor erythroid-2-related factor 2 gene expression in non-small cell lung cancer inhibits tumor growth and increases efficacy of chemotherapy. Cancer Res. *68*, 7975–7984.

Sotelo-Hitschfeld, T., Fernández-Moncada, I., and Barros, L.F. (2012). Acute feedback control of astrocytic glycolysis by lactate. Glia *60*, 674–680.

Suzuki, A., Stern, S.A., Bozdagi, O., Huntley, G.W., Walker, R.H., Magistretti, P.J., and Alberini, C.M. (2011). Astrocyte-neuron lactate transport is required for long-term memory formation. Cell *144*, 810–823.

Takimoto, M., and Hamada, T. (2014). Acute exercise increases brain region-specific expression of MCT1, MCT2, MCT4, GLUT1, and COX IV proteins. J. Appl. Physiol. *116*, 1238–1250.

Tang, F., Lane, S., Korsak, A., Paton, J.F.R., Gourine, A.V., Kasparov, S., and Teschemacher, A.G. (2014). Lactate-mediated glia-neuronal signalling in the mammalian brain. Nat. Commun. *5*, 3284.

Tian, W.-N., Braunstein, L.D., Pang, J., Stuhlmeier, K.M., Xi, Q.-C., Tian, X., and Stanton, R.C. (1998). Importance of glucose-6-phosphate dehydrogenase activity for cell growth. J. Biol. Chem. *273*, 10609–10617.

Tsouko, E., Khan, A.S., White, M.A., Han, J.J., Shi, Y., Merchant, F.A., Sharpe, M.A., Xin, L., and Frigo, D.E. (2014). Regulation of the pentose phosphate pathway by an androgen receptor-mTOR-mediated mechanism and its role in prostate cancer cell growth. Oncogenesis *3*, e103.

van Hall, G., Strømstad, M., Rasmussen, P., Jans, Ø., Zaar, M., Gam, C., Quistorff, B., Secher, N.H., and Nielsen, H.B. (2009). Blood lactate is an

important energy source for the human brain. J. Cereb. Blood Flow Metab. *29*, 1121–1129.

van Praag, H., Christie, B.R., Sejnowski, T.J., and Gage, F.H. (1999a). Running enhances neurogenesis, learning, and long-term potentiation in mice. Proc. Natl. Acad. Sci. *96*, 13427–13431.

van Praag, H., Kempermann, G., and Gage, F.H. (1999b). Running increases cell proliferation and neurogenesis in the adult mouse dentate gyrus. Nat. Neurosci. *2*, 266–270.

Vander Heiden, M.G., Cantley, L.C., and Thompson, C.B. (2009). Understanding the Warburg effect: the metabolic requirements of cell proliferation. Science *324*, 1029–1033.

Walker, T.L., Overall, R.W., Vogler, S., Sykes, A.M., Ruhwald, S., Lasse, D., Ichwan, M., Fabel, K., and Kempermann, G. (2016). Lysophosphatidic acid receptor is a functional marker of adult hippocampal precursor cells. Stem Cell Rep. *6*, 552–565.

Walker, T.L., White, A., Black, D.M., Wallace, R.H., Sah, P., and Bartlett, P.F. (2008). Latent stem and progenitor cells in the hippocampus are activated by neural excitation. J. Neurosci. *28*, 5240–5247.

Wanet, A., Arnould, T., Najimi, M., and Renard, P. (2015). Connecting mitochondria, metabolism, and stem cell fate. Stem Cells Dev. *24*, 1957–1971.

Wang, J., Cui, Y., Yu, Z., Wang, W., Cheng, X., Ji, W., Guo, S., Zhou, Q., Wu, N., Chen, Y., et al. (2019). Brain Endothelial Cells Maintain Lactate Homeostasis and Control Adult Hippocampal Neurogenesis. Cell Stem Cell *25*, 754–767.e9.

Wang, Y.P., and Lei, Q.Y. (2018). Metabolite sensing and signaling in cell metabolism. Signal. Transduct. Target Ther. *3*, 30.

Warburg, O. (1925). The metabolism of carcinoma cells. J. Cancer Res. *9*, 148–163.

Xu, S.-N., Wang, T.-S., Li, X., and Wang, Y.-P. (2016). SIRT2 activates G6PD to enhance NADPH production and promote leukaemia cell proliferation. Sci. Rep. *6*, 32734.

Xu, X., Duan, S., Yi, F., Ocampo, A., Liu, G.-H., and Belmonte, J.C.I. (2013). Mitochondrial regulation in pluripotent stem cells. Cell Metab. *18*, 325–332.

Yanamadala, V., Negoro, H., and Denker, B. (2009). Heterotrimeric G proteins and apoptosis: intersecting signaling pathways leading to context dependent phenotypes. Curr. Mol. Med. *9*, 527–545.

Yang, J., Ruchti, E., Petit, J.-M., Jourdain, P., Grenningloh, G., Allaman, I., and Magistretti, P.J. (2014). Lactate promotes plasticity gene expression by potentiating NMDA signaling in neurons. Proc. Natl. Acad. Sci. *111*, 12228–12233.

Zhang, W., and Liu, H.T. (2002). MAPK signal pathways in the regulation of cell proliferation in mammalian cells. Cell Res. *12*, 9–18.

Zheng, X., Boyer, L., Jin, M., Mertens, J., Kim, Y., Ma, L., Ma, L., Hamm, M., Gage, F.H., and Hunter, T. (2016). Metabolic reprogramming during neuronal differentiation from aerobic glycolysis to neuronal oxidative phosphorylation. Elife *5*, e13374.

iScience, Volume *24*

Supplemental Information

L-lactate exerts a pro-proliferative effect on adult hippocampal precursor cells *in vitro*

Alexandra Pötzsch, Sara Zocher, Stefanie N. Bernas, Odette Leiter, Annette E. Rünker, and Gerd Kempermann

Supplemental Information

Supplemental figures and legends

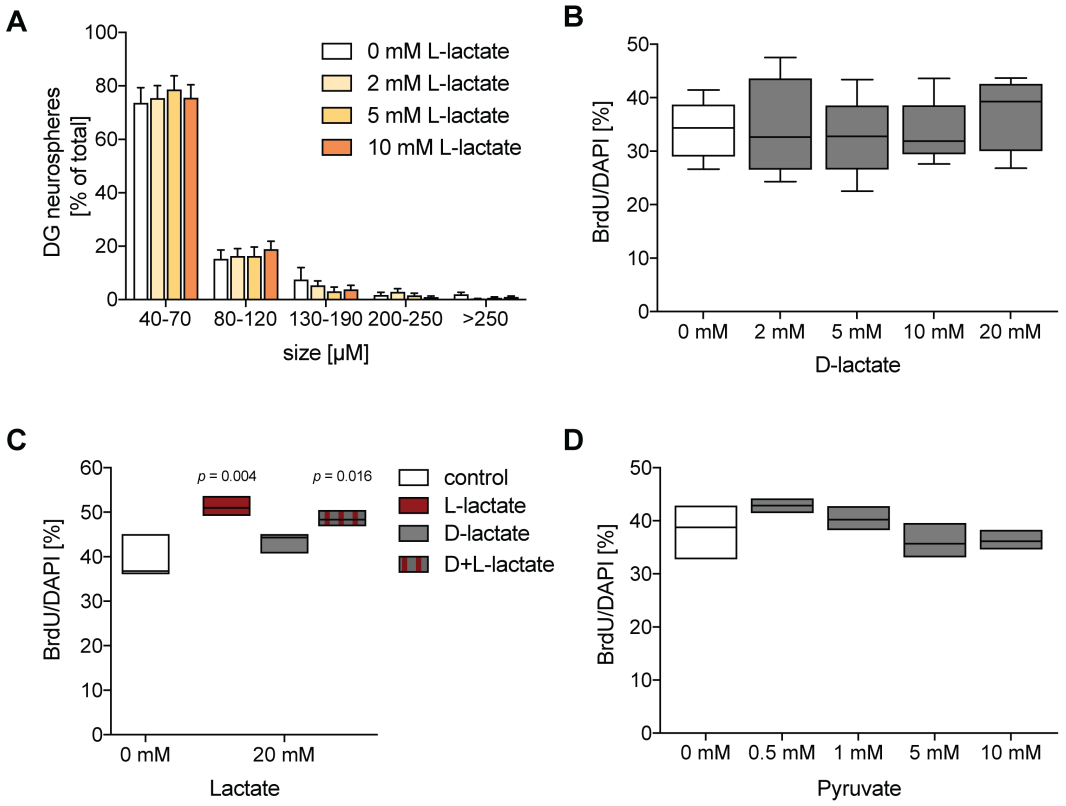

Figure S1, related to Figure 1

(A) Quantification of DG neurosphere sizes following treatment with L-lactate (n = 5).
(B) Quantification of BrdU-positive monolayer NPCs following treatment with D-lactate, stereoisomer of L-lactate (n = 5).
(C) Percentage of BrdU-positive cells following treatment with 20 mM L-lactate, D-lactate or D+L-lactate in comparison to control cells (n = 3).
(D) Quantification of BrdU-positive cells after treatment with increasing concentration of pyruvate.
Statistics: one-way ANOVA with Dunnett's *post hoc*.

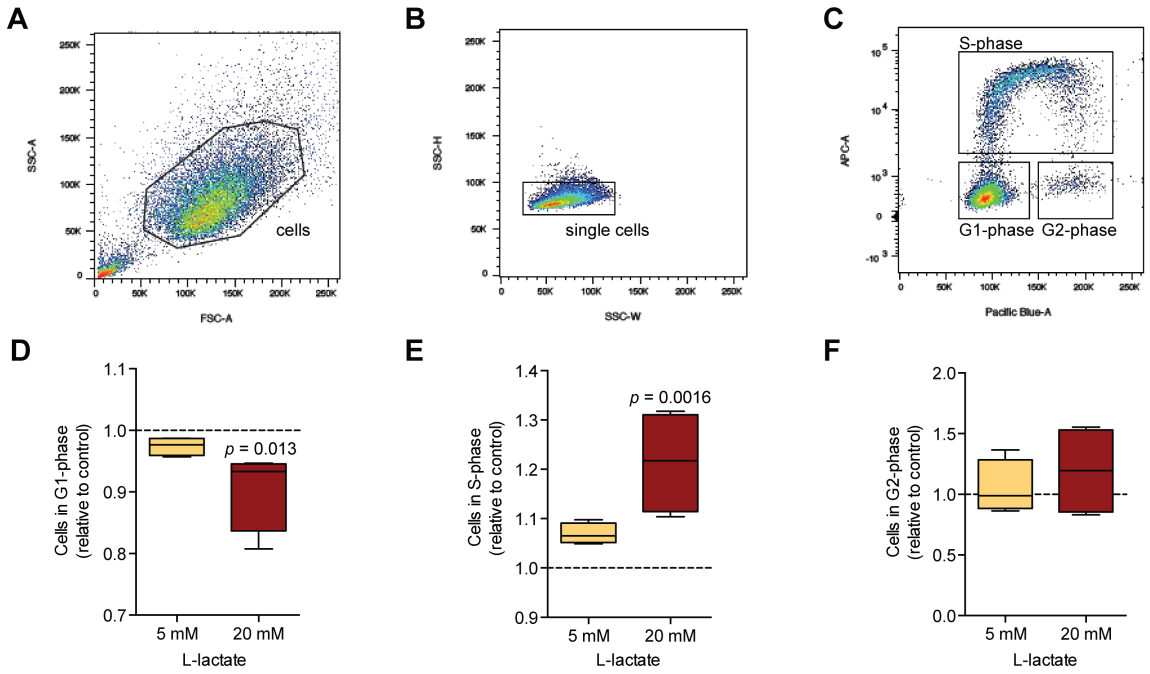

Figure S2, related to Figures 1 and 6

(A – C) Gating strategy for determination of cell cycle phases using EdU (APC-A) and DAPI (Pacific Blue-A).

(D) Relative amount of L-lactate treated NPCs in G1-phase relative to control (n = 4).

(E) Relative amount of L-lactate treated NPCs in S-phase relative to control (n = 4).

(F) Relative amount of L-lactate treated NPCs in G2-phase relative to control (n = 4)

Statistics: one-way ANOVA with Dunnett's *post hoc*.

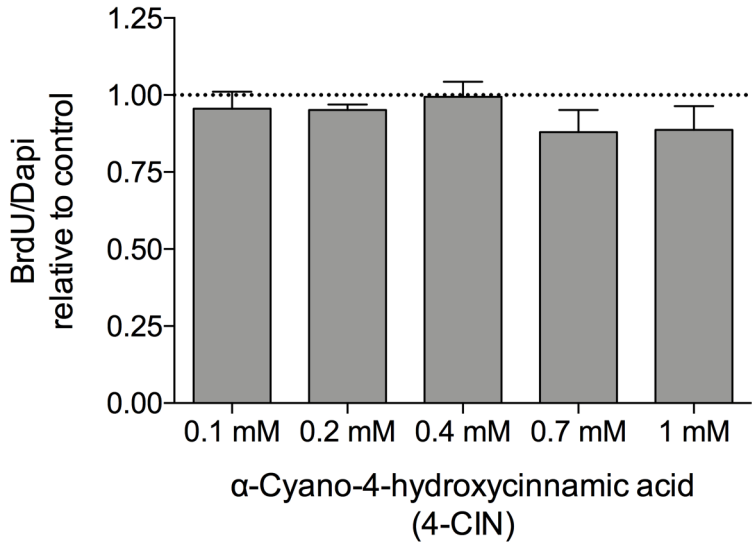

Figure S 3, related to Figure 4
Ratio of BrdU-positive cells treated with increasing concentrations of 4-CIN relative to control NPCs (n = 3). Data are presented as mean +/- SEM.

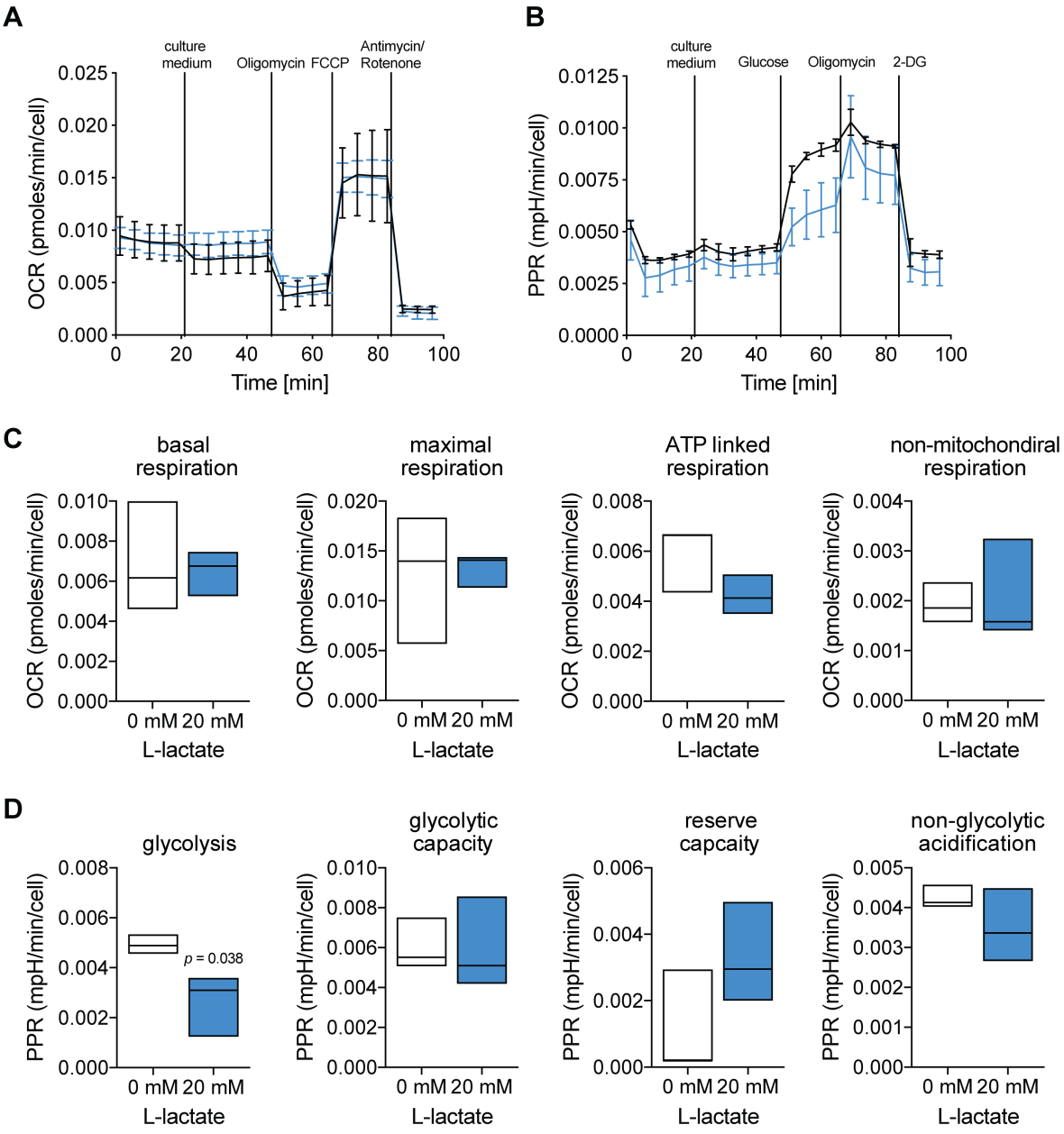

Figure S 4, related to Figure 5

(A) Glycolytic behavior of NPCs following pre-incubation with L-lactate (0 mM or 20 mM) for 24 h and subsequent manipulation of metabolism glucose, oligomycin and 2-DG using the Seahorse Analyzer XF96. Data are normalized to total cell numbers and expressed as PPR (n = 3).

(B) Mitochondrial respiration of NPCs presented as OCR and normalized to total cell numbers in NPCs pre-treated with L-lactate (0 mM or 20 mM) for 24 h and subsequently treated with oligomycin, FCCP and antimycin/rotenone using the Seahorse Analyzer XF96 (n = 3).

(C) Rate of glycolysis, glycolytic capacity and reserve (n = 3).

(D) Rate of basal respiration, maximal respiration and ATP linked respiration (n = 3).

Data are presented as mean +/- SEM (A, C, E). Statistics: unpaired Students t-test.

Transparent Methods

Animals

Mice (C57BL/6JRj, 8 week-old, female) were housed on a 12 h light/dark cycle in standard cages with food and water provided *ad libitum* in the animal facility of the Center for Regenerative Therapies TU Dresden (CRTD). All animal experiments were conducted in agreement with the local authorities (Landesdirektion Sachsen) and in accordance with the applicable directive of the European Union and national regulations (Tierschutzgesetz) under the file number TA 24-9168.24-1/2013-16.

Compounds

NPCs were treated with the compounds listed below, which were dissolved in ddH_20 unless otherwise indicated: Sodium-L-lactate (L7022) and Sodium-D-lactate (71716, both Sigma), Pyruvate (11360070, Gibco), 4-CIN (DMSO; C2020, Sigma), 3,5-DHBA (D110000, Sigma), LY294002 (DMSO; 9901, CellSignaling).

Neurosphere cultures

Single cells were isolated from the dentate gyrus (DG) and the subventricular zone (SVZ), of 8-week old C57BL/6Rj mice as previously described (Bernas et al., 2017; Walker and Kempermann, 2014). Briefly, mice were deeply anesthetized with isoflurane and killed, their brains removed and the DG and SVZ were microdissected. DG tissue was enzymatically digested using the Neural Tissue Dissociation Kit (Miltenyi) according to the manufacturer's instructions and the cells washed in HBSS (GE Healthare). SVZ tissue was digested for 7 min using 0.05 % Trypsin-EDTA and the enzymatic reaction was stopped using Trypsin inhibitor containing DNase I. The cell suspension was centrifuged at 300 x g for 5 min and filtered through a 40 µm cell strainer. The cells were resuspended in neurobasal (NB) proliferation medium (with B-27 supplement, penicillin/streptomycin, GlutaMAX; all Gibco) supplemented with 20 ng/ml EGF (Peprotech), 20 ng/ml FGF2 (Peprotech) and L-lactate. The cells were seeded at a density corresponding to the DGs and SVZs of one mouse per plate across a 96-well plate in a volume of 200 µl per well resulting in an average of one sphere per well. Neurospheres were incubated at 37°C and 5 % CO_2 for 7 days (SVZ) or 10 days (DG) without further media change or additional L-lactate supplementation. Subsequently neurospheres of all wells of each plate were quantified and their size was measured using the Olympus CKX41 inverted microscope with a 10x objective and an ocular scale.

For neurosphere differentiation, approximately 12 neurospheres were selected randomly and plated onto poly-D-lysine (PDL; 5 µg/ml) and laminin (5 µg/ml)-coated coverslips in a 24-well

plate containing NB medium without growth factors. After 7 days, cells were washed with PBS and fixed with 4 % paraformaldehyde (PFA) for 10 min at room temperature (RT).

Adherent monolayer cultures

For monolayer cultures, NPCs established in our laboratory were thawed from frozen stocks, resuspended in NB proliferation medium containing 10 ng/ml EGF and 10 ng/ml FGF2 and seeded into PDL/laminin-coated vessels.

To assess proliferation, NPCs were plated onto PDL/laminin-coated coverslips in 24-well plates. After treatment with a compound for 48 h, cells were subjected to BrdU (final conc. 10 µM) for 2 h, washed with PBS and fixed with 4 % PFA. For immunocytochemistry of membrane proteins, proliferating NPCs were fixed with ice-cold acetone and methanol (1:1) at -20°C for 10 min instead.

For differentiation of adherent monolayer cells, NPCs were seeded onto PDL/laminin-coated coverslips in 24-well plates under proliferation conditions. After 48 h, cells were differentiated for 5 days in NB medium without EGF and FGF2. Subsequently, cells were washed with PBS and fixed with 4 % PFA.

Propidium iodide (PI)-based cell cycle analysis

NPCs were treated with L-lactate and, after 48 h, cells were detached and fixated with 70 % ice-cold ethanol for 1 h at 4°C, After washing, cells were resuspended in PI solution (50 µg/ml) containing RNase A (100 µg/ml) and incubated for 1 h in the dark at RT. PI signal was analyzed with the Accuri C6 flow cytometer and analyzed using FlowJo. First, we excluded cellular debris from the analysis by side scatter area (SSC-A) and forward scatter area (FSC-A). Secondly, single cells were separated from doublets by forward scatter height (FSC-H) and FSC-A and, lastly, the signal in the PI channel (Cy5) was plotted against the cell count. From the resulting histograms, distribution of cells into G0/1, S and G2 phase was determined.

Cell tracking

NPCs were seeded in NB proliferation medium into PDL/laminin coated 24-well glass bottom plates and supplemented with L-lactate. Time-lapse imaging was performed for 3.5 days (acquisition every 5 min, 20 ms exposure time) utilizing an inverted, motorized spinning disc microscope (Zeiss Axio Observer.Z1) equipped with a 10x objective (Zeiss) and an integrated incubation chamber to control temperature and CO_2 at 37°C and 5 %, respectively. Three open-source software tools were combined (CellTracker, CellProfiler and R; (Carpenter et al., 2006; Scherf et al., 2012; Team, 2014)) to enable semi-automated (user-supervised) tracking of single cells. Following automatic tracking of single cells, cell

tracks were manually verified and corrected using CellTracker. With CellTracker, four labels can be assigned to each tracked cell: 'Cell died', 'cell divided', 'cell was tracked till the end' and 'cell was lost'. Thereby, the number of dividing cells can be quantified and further analyzed by assigning 'daughter cells' resulting from cell division to their respective 'mother cell' resulting in the generation of lineage trees that grow with each cell division within that lineage. The time between two cell divisions within one lineage tree can then be quantified as the generation time. The generation time of tracked cells was calculated using R.

Annexin V/PI cell death assay

L-lactate treated NPCs were detached, washed in ice-cold PBS and 1 million cells were subjected to Annexin V and PI treatment according to the manufacturer's instructions (Invitrogen). Strained cells were analyzed with the Accuri C6 flow cytometer and data were analyzed with FlowJo v10.

BMP4 quiescence assay

To induce quiescence, medium of proliferating NPCs was exchanged to medium supplemented with 20 ng/ml FGF2 and 50 ng/ml BMP4 (R&D Systems) as described by (Martynoga et al. 2013). After 4 days, quiescent cells were treated with L-lactate or passaged (Walker and Kempermann 2014) and seeded into medium containing 10 ng/ml EGF, 10 ng/ml FGF2 and L-lactate to induce proliferation. Proliferation was assessed using BrdU after 4 days.

Glucose medium analysis

To analyze glucose consumption, cell medium of L-lactate-treated and control cells was collected after 24 h and 48 h of culture and stored at -80°C. Simultaneously, cell numbers were calculated at each time point by automatic quantification (Countess II, Invitrogen) using trypan blue. Glucose concentration in the culture medium was determined with the Amplex Red Glucose kit (A22189, Invitrogen). For that purpose, samples were pre-diluted 1:200 in assay buffer and further analyzed according to the manufacturer's instructions. Results for each time point were normalized to the respective cell numbers.

Glucose-6-phosphate dehydrogenase (G6PD) activity assay

Following L-lactate treatment for 6 h, 24 h and 48 h, NPCs were harvested in ice-cold PBS and rapidly homogenized on ice. The G6PD assay was performed according to the manufacturer's instructions (MAK015, Sigma). In addition, protein concentrations were determined with a Bradford Protein Assay (BCA) for normalization of G6PD data to total protein.

Seahorse XF96 assay

Real-time measurements of glycolysis (proton pump rate, PPR) and oxidative phosphorylation (oxygen consumption rate, OCR) were obtained with the Seahorse XF96 Analyzer (Seahorse Biosciences). Briefly, NPCs were seeded into a PDL/laminin coated Seahorse culture plate at a density of 8000 cells/well and cultured for 24 h under proliferation conditions. Before analysis of the PPR, culture medium was removed and exchanged for assay medium (DMEM with 2 mM L-glutamine, 0.227 mM pyruvate, B27 supplement, 10 ng/ml EGF and FGF2, pH 7.4) depriving cells of glucose for 1 h. Following baseline measurements, NPCs were stimulated using the compounds provided in the XF Glycolysis Stress Test Kit (Seahorse Bioscience) by successive injection of L-lactate (20 mM) or medium without L-lactate (0 mM), glucose (10 mM), oligomycin (1 µM) and 2-DG (2-deoxyglucose; 50 mM). For analysis of OCR using the XF Cell Mito Stress Test Kit (Seahorse Bioscience), culture medium was exchanged before the assay for assay medium containing glucose (25 mM). Baseline measurements were carried out followed by injection of L-lactate (20 mM) or medium without L-lactate (0 mM), oligomycin (1 µM), carbonyl cyanide 4-(trifluoromethoxy) phenylhydrazone (FCCP) (2 µM), and rotenone/antimycin A (0.5 µM). At the end of each assay, cells were fixed with 4 % PFA and cell numbers were automatically quantified. All data were then normalized to the total cell number. Parameters were calculated as described in the respective user guides of the assays.

Generation and analysis of HCAR1-KO NPCs

Cloning of constructs for CRISPR-Cas9-based deletion of Hcar1

CRISPR-Cas9 constructs were generated according to Ran et al. (Ran et al. 2013). Briefly, sgRNAs were designed to target the beginning (Hcar1_up: GGTCGTGCTGTCTCATCGAG) and end (Hcar1_down: GTTCCCAGAGGCCATCTGAC) of the only exon of *Hcar1* using an online CRISPR Design Tool (http://www.e-crisp.org/E-CRISP/) with gene sequences downloaded from Ensembl (http://www.ensembl.org/Mus_musculus/). SgRNAs were annealed and phosphorylated by incubating 1 µl of top and bottom strand oligonucleotides (100 µM) with 5 units T4 Polynucleotide Kinase (Thermo Fisher Scientific) in 1 x T4 DNA Ligase Buffer (Thermo Fisher Scientific) at 37 °C for 30 min followed by 95 °C for 5 min and ramp down to 25 °C at 5 °C/min. Hybridized sgRNAs were cloned into pSpCas9(BB)-2A-Puro V2.0 (Addgene plasmid ID: 62988) in a single reaction containing 100 ng plasmid, 2 µl of diluted sgRNAs (1:250), 1 x FastDigest Buffer (Thermo Fisher Scientific), 1 µl dithiothreitol (10 mM), 10 units FastDigest BpiI (Thermo Fisher Scientific) and 2.5 units T4 DNA Ligase (Thermo Fisher Scientific). This restriction and ligation reaction was incubated for 6 cycles at 37 °C for 5 min followed by 23 °C for 5 min and transformed into chemically competent

Escherichia coli TOP10. Plasmids were isolated from single bacteria colonies using GeneJET Plasmid Miniprep Kit (Thermo Fisher Scientific). SgRNA insertion was verified by Sanger sequencing with primers targeting the U6 promoter of pSpCas9(BB)-2A-Puro V2.0.

Transfection of neural precursor cells

Plasmids SpCas9(BB)-2A-Puro V2.0 containing sgRNAs were purified using EndoFree Plasmid Maxi Kit (QIAGEN) and transfected into NPCs using Lipofectamin 3000 Reagent (Thermo Fisher Scientific). To delete *Hcar1*, the two sgRNAs Hcar1_up and Hcar1_down were simultaneously transfected. Control cells were transfecting with a sgRNA targeting lacZ (GTGCGAATACGCCCACGCGAT). Adherent monolayer cultures were transfected at p7 when cells reached a confluence of 70 %. For transfections, 480 µl of Opti-MEM reduced serum medium (Thermo Fisher Scientific) were mixed with 10 µl Lipofectamin 3000 Reagent, 8 µl of P3000 Reagent and 15 µg of each plasmid. The mix was incubated at room temperature for 20 min and added to NPCs cultured in 4.5 ml of proliferation medium. Transfected cells were selected by incubation in proliferation medium containing puromycin (2 µg/ml) for 24 h, after which cells were expanded in proliferation medium.

Generation of monoclonal cell lines

Puromycin-selected cells were diluted to a density of 100 cells per 20 ml proliferation medium and were distributed into single wells of a 96-well plate (200 µl/well). NPCs were incubated for 14 days to allow neurosphere formation. Single neurospheres were transferred to a PDL/laminin-coated 96-well plate and dissociated by pipetting up and down with a conventional 100 µl pipette tip. Cell lines were expanded over several passages.

Genotyping of cell lines

Genomic DNA was isolated from the individual cell lines using QIAamp DNA Micro Kit (QIAGEN) according to the manufacturer's instructions. Gene fragments flanking the target site of the respective CRISPR-Cas9 constructs were amplified using Phusion DNA polymerase (Thermo Fisher Scientific) with primers *Hcar1* forward (AGTTTCTCTCGTGGGTGCAG) and *Hcar1* reverse (TGCTTGCCTGGCTCGAATAA).

Proliferation assay

Cells were treated with L-lactate for 48 h, subsequently incubated with EdU for 2.5 h, processed using Click-iT™ EdU Alexa Fluor™ 647 Flow Cytometry Assay Kit (Thermo Fisher Scientific) and analyzed using a BD LSR II. At least 50.000 cells were recorded. Data was analyzed using FlowJo v10.

Immunocytochemistry and quantification

Fixed cells were permeabilized (0.1 % TritonX-100) and unspecific antibody binding was blocked for 1 h using 10 % donkey serum. In case of BrdU treatment, cells were pretreated with 0.9 % NaCl, incubated with 1 M HCl (30 min at 37°C) and washed with 0.5 M borate buffer followed by PBS before proceeding to permeabilization. For staining of membrane proteins, membrane permeabilization was omitted. Following blocking, cells were incubated with the following primary antibodies diluted in 3 % donkey serum for 2 h at RT: rat anti-BrdU antibody (1:500, 2 h at RT; OBT0030, Bio-Rad), goat anti-MCT2 (1:500; sc14926, Santa Cruz), rabbit anti-MCT4 (1:500; sc50329, Santa Cruz), rabbit anti-GPR81-s296 (1:500), mouse anti-Nestin (1:500; 611658, BD), rabbit anti-GFAP (1:500; Z0334,, Agilent Technologies), mouse anti-β-Tubulin (1:2000; G7121, Promega), mouse anti-MAP2ab (1:500; M1406, Sigma). After washing with PBS, cells were incubated with secondary antibodies for 1 h in the dark at RT: anti-rat Alexa488 secondary antibody (1:500, 1 h at RT; Dianova), anti-rabbit Alexa 488 and Alexa 568 (1:500; Fisher Scientific), anti-goat Alexa 568, anti-mouse Cy3 and anti-mouse Alexa 588 (1:500; Dianova). Nuclei were detected with DAPI (1:4000, 10 min at RT; Thermo Fisher). Coverslips were mounted with Aqua-Poly/Mount (Polysciences Inc.) or, in case of confocal imaging, with Vectashield mounting medium (Vector Laboratories). For cell quantification (BrdU, differentiation), 10 fields of view (FOV) from 2 coverslips per treatment group of each experiment were imaged with an ApoTome (Axio Imager.M2; Zeiss) using a 20x objective (Zeiss). FOV were selected in the DAPI channel to prevent bias. Cells were quantified manually using the cell counter tool in ImageJ. For qualitative assessment of MCTs and HCAR1, images were obtained using the LSM 780 NLO confocal laser-scanning microscope equipped with a 100x oil objective (Zeiss). Images were processed with ImageJ.

RNA isolation and RT-PCR

RNA was isolated from adherent monolayer cells using TRI reagent and resuspended in RNAse-free water. A total of 1 µg RNA was used for cDNA generation. Briefly, samples were digested with 1 U/µl DNase1 for 15 min at RT, stopped by EDTA and heating to 65°C for 10 min. Synthesis of cDNA was performed with the Roche Transcriptor First Strand cDNA Synthesis Kit using anchored oligo(dT)18 and random hexamer primer according to the manufacturer's instructions (cycling condition: 10 min at 25°C, 30 min at 55°C and 5 min at 85°C).

Quantitative PCR (qPCR)

Synthesized cDNA was used to perform qPCR with SsoFast EvaGreen supermix (Biorad) on a CFX96 (Biorad) system (cycling conditions: initial denaturation 3 min at 95°C, denaturation

10 sec at 95°C, annealing/extension 30 sec at 60.5°C, melting curve 5 sec at 65°C to 95°C). Primers were designed using NCBI tool in such a way, that the amplicon would not exceed 200 bp and span an exon-exon region (primers 5´- 3´: *Slc16a1* forward CGCGAGACACACATAACGATAC, reverse AAGGCTCCGACTAACACTGC; *Slc16a3* forward GTCATCACTGGCTTGGGTCT, reverse AATAGGGCGACGCTTGTTGA; *Slc16a7* forward ACTCAGCTTTGGTGGTCTACG, reverse CAATTTACCAGCCAGAGGAGGG; *β-actin forward* ACTGTCGAGTCGCGTCC, reverse TCATCCATGGCGAACTGGTG). Results were analyzed using the ΔΔCt method. To verify amplicon size, qPCR products were additionally analyzed by gel electrophoresis.

Western blot

NPCs were harvested and membrane proteins were isolated using the Mem-PER^{TM} Plus Membrane Protein Extraction Kit (Thermo Scientific) supplemented with protease inhibitor (Serva) according to the manufacturer's instructions. For cytosolic protein isolations, NPCs were harvested in lysis buffer (RIPA) containing protease (Serva) and phosphatase (Roche) inhibitor cocktails and protein concentrations were determined with BCA assays (Thermo Scientific) according to the manufacturer's instructions. Proteins (15 µg) were heated for 5 min at 95°C, separated on a 12 % polyacrylamide gel by SDS-PAGE and transferred onto nitrocellulose membranes at 350 mA for 90 min. Membranes were blocked with 5 % non-fat milk in TBS-Tween for 1 h at RT, washed in TBS-Tween and incubated with the following primary antibodies diluted in 5 % BSA in TBS-Tween at 4°C over night: goat anti-MCT2 (1:500; sc14926, Santa Cruz), rabbit anti-MCT4 (1:500; sc50329, Santa Cruz), rabbit anti-GPR81-s296 (1:500), rabbit anti-p44/42 MAPK (ERK1/2) (1:1000; #4695), rabbit anti-phospho-p44/52 MAPK (ERK1/2 Thr202/Tyr204) (1:2000; #4370), rabbit anti-Akt (1:1000; #4691), rabbit anti-phospho-Akt (Ser473) (1:2000; #4060; all CellSignaling). Primary antibodies were detected with polyclonal anti-rabbit IgG conjugated with IRDye 680 or anti-goat IgG conjugated with IRDye800 in 5 % non-fat milk in TBS-Tween (1:10000; LI-COR). Protein bands were visualized utilizing the Odyssey Infrared Imaging System (LI-COR) and bands were quantified with ImageJ.

Data analysis

Data were analyzed using GraphPad prism and visualized as boxplots or bar graphs (mean +/- SEM) unless indicated otherwise. For analysis of statistical significance, one-way ANOVA and, if applicable, Dunnett's *post hoc* test, two-way ANOVA and Fisher's LSD *post hoc* or unpaired Student's *t*-test were employed. Differences between datasets were deemed statistically significant at $p < 0.05$.

References

Bernas, S., Leiter, O., Walker, T., and Kempermann, G. (2017). Isolation, Culture and Differentiation of Adult Hippocampal Precursor Cells. Bio-Protocol *7*.

Carpenter, A.E., Jones, T.R., Lamprecht, M.R., Clarke, C., Kang, I.H., Friman, O., Guertin, D.A., Chang, J.H., Lindquist, R.A., Moffat, J., et al. (2006). CellProfiler: image analysis software for identifying and quantifying cell phenotypes. Genome Biol *7*, R100.

Scherf, N., Franke, K., Glauche, I., Kurth, I., Bornhäuser, M., Werner, C., Pompe, T., and Roeder, I. (2012). On the symmetry of siblings: automated single-cell tracking to quantify the behavior of hematopoietic stem cells in a biomimetic setup. Exp Hematol *40*, 119-130.e9.

Team, R.C. (2014). R: A language and environment for statistical computing.

Walker, T.L., and Kempermann, G. (2014). One mouse, two cultures: isolation and culture of adult neural stem cells from the two neurogenic zones of individual mice. Journal of Visualized Experiments : JoVE e51225.